



CATÓLICA
UNIVERSIDADE CATÓLICA PORTUGUESA | PORTO
Escola Superior de Biotecnologia

NOVEL HYALURONAN-BASED HYDROGELS OBTAINED BY
SUPRAMOLECULAR CROSSLINKING WITH PEPTIDES

by

Ana Luísa de Oliveira Leite Faria

January 2017



CATÓLICA
UNIVERSIDADE CATÓLICA PORTUGUESA | PORTO
Escola Superior de Biotecnologia

NOVEL HYALURONAN-BASED HYDROGELS OBTAINED BY
SUPRAMOLECULAR CROSSLINKING WITH PEPTIDES

Thesis presented to *Escola Superior de Biotecnologia* of the *Universidade Católica Portuguesa* to
fulfill the requirements of Master of Science degree in Biomedical Engineering.

by

Ana Luísa de Oliveira Leite Faria

Place: Queen Mary University of London- School of Engineering and Materials Science (SEMS)

Supervision: Dr. Helena Azevedo

Co-supervision: Elham Radvar

January 2017

Resumo

Nos últimos anos, biomateriais formados por auto-organização molecular constituídos por péptidos têm vindo a ser desenvolvidos como solução a vários desafios médicos. Os péptidos são interessantes unidades moleculares, uma vez que a partir da combinação de diferentes aminoácidos é possível obter biomateriais com propriedades específicas de bastante interesse em diversas áreas, como por exemplo, engenharia de tecidos e medicina regenerativa. Neste projeto, hidrogéis à base de ácido hialurónico foram desenvolvidos a partir de interações supramoleculares com diferentes péptidos, para aplicação biomédica. Como tal, péptidos com diferentes sequências, possuindo um resíduo carregado positivamente numa extremidade e um resíduo aromático na outra extremidade da sequência, foram sintetizados para formarem interações supramoleculares com o ácido hialurónico e interações entre os anéis aromáticos dos péptidos. A massa dos péptidos sintetizados foi confirmada por Espectrometria de Massa com Ionização por Electrospray, a sua pureza por Cromatografia Líquida de Alta Eficiência e a estrutura secundária por espectroscopia de dicroísmo circular. No sentido de investigar a formação de hidrogéis, os péptidos, em pó ou em soluções de diferentes concentrações a pH neutro e ácido, foram combinados com soluções de 1% e 2% de ácido hialurónico com diferentes massas moleculares, usando diferentes estratégias. Era esperada a formação de hidrogéis através de interações eletrostáticas entre os resíduos positivos do péptido e o ácido hialurónico (carga negativa), e ainda π - π stacking entre os anéis aromáticos dos resíduos dos péptidos. Os hidrogéis obtidos foram caracterizados por Microscopia de Varrimento Eletrónico, tendo revelado estruturas compostas por uma rede de nanofibras. A concentração da solução de ácido hialurónico e a sua massa molecular, bem como a sequência do péptido, mostraram ter efeito na densidade e organização das fibras.

Abstract

In recent years, self-assembled biomaterials using peptides as building blocks have been developed as a solution for several medical challenges. Peptides offer a great diversity of biochemical properties and, through the combination of different amino acids, it is possible to produce a variety of peptide-based structures with specific proprieties with interest for regenerative medicine and tissue engineering. In the present project, novel hyaluronan base hydrogels obtained by supramolecular crosslinking with peptides were developed for biomedical application. Thus, different designs of peptides, containing a positively charged residue at one end and an aromatic residue at other end, were synthesized to form supramolecular interactions with hyaluronic acid (HA). The mass of the synthesised peptides was confirmed by Electrospray Ionization Mass Spectrometry (ESI-MS), their purity by High Performance Liquid Chromatography (HPLC) and their secondary structure by Circular Dichroism (CD) spectroscopy. In order to investigate gel formation, the peptides, in powder form and in solution of different concentrations at neutral and acidic pH, were combined with 1% and 2% w/v HA solutions of different molecular weights, following different strategies. Observation of gel formation was expected through electrostatic interactions between the positively charge residue of the peptide with HA (negatively charged) and π - π stacking between aromatic residues of the peptides. The resulted hydrogels were characterized by Scanning Electron Microscopy (SEM), revealing a network of nanofibrous structures. The concentration of the HA solutions, different molecular weights HA and the peptide design showed to have an effect on the density, organization and packing of the fibers.

Acknowledgments

I'm very grateful to my supervisor Dr.Helena Azevedo for supporting and advising me. As well as, for providing me with this opportunity of being part of MHAtriCell's group, who I'm grateful too. I wish to thank my co-supervisor Elham Radvar for her immense backing, and endless assistance and guidance. To my family, boyfriend and friends, many thanks for their continued motivation and neverending encouragement. Lastly, I would like to thank Professor Dr.João Paulo Ferreira and Escola Superior de Biotecnologia of the Universidade Católica Portuguesa.

Table of Contents

Resumo	v
Abstract.....	vii
Acknowledgments	ix
List of figures	xiii
List of tables	xv
List of abbreviations.....	xvii
CHAPTER 1: Introduction	1
1) Amino acids and peptides	1
1.1) Amino acids	1
1.2) Peptides.....	4
1.3) Peptide synthesis.....	6
2) Molecular self-assembly	7
2.1) Molecular self-assembly and supramolecular interactions.....	7
2.2) Peptide self-assembly	9
3) Hyaluronic acid	11
4) Aim.....	12
CHAPTER 2: Materials and Methods	15
1) Peptide synthesis	15
2) Peptide Purification and Characterization	17
2.1) ESI-MS	17
2.2) HPLC	18
2.3) CD spectroscopy	19
3) Peptide-HA hydrogels preparation	20
4) Peptide-HA hydrogels characterization	24
4.1) SEM.....	24
CHAPTER 3: Results and Discussion	27
1) Peptide synthesis	27
2) Peptide purification and characterization	28
2.1) ESI-MS	28
2.2) HPLC	32
2.3) CD.....	34
3) Peptide-HA hydrogels preparation	38
4) Peptide-HA hydrogels characterization	42
4.1) SEM.....	42
CHAPTER 4: Conclusion and future work	49
1) Conclusion	49
2) Future work.....	49

APPENDIX.....	51
1) Yield Calculations	51
References	52

List of figures

Figure 1.1- General structure of an amino acid (Nelson & Cox, 2008).	2
Figure 1.2- Formation of a peptide bond (Chatterjea & Shinde, 2011).	5
Figure 1.3- Levels of structures in proteins (Nelson & Cox, 2008).	6
Figure 1.4- Possible π - π stacking geometries: a) parallel displaced, b) T-shape, c) parallel staggered and d) herringbone (Gazit, 2002).	8
Figure 1.5- Macroscopic and microscopic analysis of the hydrogel obtained by self-assembled of the Fmoc-diphenylalanine peptide. a) The Fmoc-Phe-Phe hydrogel in the inverted cuvette; b) the letters TAU were written by injecting the gel from a syringe onto a plastic substract; c) transmission electron microscopy image of fibrous scaffold; d) high resolution SEM image of the scaffold fibrils. Adapted from (Mahler et al., 2006).	10
Figure 1.6- Chemical structure of Hyaluronan: three repeating units for the disaccharide GlcA-GlcNAc are shown (Jiang et al., 2007).	11
Figure 1.7- SEM images of self-assembled membranes with 1% (w/v) HA and 2% (w/v) K-PA, showing the HA side (C1), peptide side (C2) and cross section (C3, C4) (Ferreira, Marques, et al., 2013).	12
Figure 2.1- Gel formation investigation for peptide Ac-K ₂ G ₅ F-CONH ₂ with 10% (w/v).	21
Figure 2.2- Gel formation investigation for the peptide Ac-KG ₅ F-CONH ₂	22
Figure 2.3- Gel formation investigation for peptide Ac-KG ₅ F ₃ -CONH ₂	23
Figure 2.4- Gel formation investigation for peptide Ac-K ₃ G ₅ F ₃ -CONH ₂	23
Figure 3.1- CD standard curve: 1) α -helix, 2) β -sheet and 3) random coil (Greenfield & Fasman, 1969).	32
Figure 3.2- Ac-K ₂ G ₅ F-CONH ₂ gel formation results: soft gel.	34
Figure 3.3- Mass-spectroscopy analysis of the synthesised peptides.	37
Figure 3.4- HPLC analysis before and after purification for the synthesised peptides.	37
Figure 3.5- CD spectroscopy analysis for the synthesised peptides.	38
Figure 3.6- Gel formation investigation results for Ac-KG ₅ F ₃ -CONH ₂	39
Figure 3.7- Gel formation results for Ac-KG ₅ F ₃ -CONH ₂ with 2% and 1% HA solution.	41
Figure 3.8- Gel formation results for Ac-K ₂ G ₇ F ₄ -CONH ₂	42
Figure 3.9- SEM images of Ac-KG ₅ F ₃ -CONH ₂ hydrogels microstructure for 2% HA (700, 200 and 20 kDa) and 1% HA (700, 200, 60 and 20); [A] one side, [B] other side, [C] and [D] cross-section.	46

Figure 3.10- SEM images for Ac-K₂G₇F₄-CONH₂ hydrogels microstructure for 20% w/v and 2% HA: 700, 200 and 60 kDa; [A] one side, [B] other side, [C] and [D] cross-section..... 48

List of tables

Table 1.1- Structure and properties of the twenty natural amino acids. Adapted from (Mendes et al., 2013).....	2
Table 2.1- Peptides sequences, chemical structure, molecular weight and synthesis scale.....	16
Table 2.2- Gradient used for analysing the peptides	19
Table 2.3- CD samples preparation: concentration and pH.	19
Table 2.4- Gel formation investigation for peptide NH ₂ -KG ₂ F-CONH ₂	20
Table 2.5- Gel formation investigation for peptide Ac-K ₂ G ₅ F-CONH ₂	21
Table 2.6- Gel formation investigation for peptide Ac-K ₂ G ₅ F-CONH ₂ in powder form.....	21
Table 2.7- Gel formation investigation for the peptide Ac-KG ₅ F-CONH ₂ in powder form.	22
Table 2.8- Gel formation investigation for peptide Ac-KG ₅ F ₃ -CONH ₂ in powder form.....	23
Table 2.9- Gel formation investigation for peptide Ac-K ₃ G ₅ F ₃ -CONH ₂ in powder form.	24
Table 2.10- Gel formation investigation for the peptide Ac-K ₂ G ₇ F ₄ -CONH ₂ in powder form.	24
Table 3.1- Solubility, mass after purification and yield of the synthesized peptides.	27
Table 3.2- Possible m/z of the synthesised peptides.	28

List of abbreviations

A	Adenine
ACN	Acetonitrile
Boc	tert-Butoxycarbonyl
C	Cytosine
CD	Circular Dichroism
DCM	Dichloromethane
DIC	Diisopropylcarbodiimide,
DMF	Dimethylformamide
ds	double-stranded
ECM	Extracellular matrix
EI	Electron Impact
ESI	Electrospray Ionization
ESI-MS	Electrospray Ionization Mass Spectrometry
FAB	Fast Atom Bombardment
Fmoc	9-fluorenylmethoxycarbonyl
G	Guanine
GAGs	Glycosaminoglycan
GlcA	Glucuronic Acid
GlcNAc	N-acetyl-D-glucosamine
HA	Hyaluronic acid
HOBT	1-Hydroxybenzotriazole Hydrate
HPLC	High-Performance Liquid Chromatography
MS	Mass Spectrometry
PA	Peptide Amphiphiles
PBS	Phosphate buffered saline
PI	Photoionization
PIP	Piperidine
RP-HLPC	Reversed-Phase High Performance Liquid Chromatography
SEM	Scanning Electron Microscopy
SPPS	Solid Phase Peptide Synthesis
SQ	Single Quadrupole

T	Thymine
TFA	Trifluoroaceticacid
TIS	Triisopropylsilane
UV	Ultraviolet

CHAPTER 1 : Introduction

Regenerative medicine and tissue engineering are emerging fields that provide solutions for several medical challenges facing ageing societies. Associated with the ageing process is the degeneration of tissues and the degradation of their extracellular matrix (ECM) over time. The ECM provides a scaffold that supports the organization of tissues and controls the crucial functions of cells: cell shape, cell migration, cell growth and differentiation (Hay, 2013). Some studies demonstrated that some essential proteins in the ECM are responsible for tissue organization and development (Fournier & Strittmatter, 2001; Hynes & Lander, 1992). Thus, the presence or absence of these proteins may influence the ability of tissue regeneration. The need for tissue repair and regeneration has motivated the development of novel biomaterials and scaffolds that mimic the structure of the ECM (Holmes, 2002). The generation of many biological structures, ranging from proteins and nucleic acids to viruses and cell membranes occurs through a self-assembly process. This process is the spontaneous organization of dispersed molecular units into ordered structures, due to their mutual interactions (Mendes et al., 2013). The self-assembly of peptides is becoming increasingly important in developing novel biomaterials. Peptides are versatile building blocks for self-assembly due to their characteristic and chemical structure that can be utilized in producing a variety of structures in the range of nano-or micrometres, thus recreating some of the architectural features of the natural ECM (Ferreira, Reis, et al., 2013). Furthermore, peptides offer a great diversity of biochemical properties such as specificity, intrinsic bioactivity and biodegradability (Mendes et al., 2013). As their chemical structure is defined, peptides can self-assemble with other natural or synthetic materials to form structures with different molecular configurations that can be used in several biomedical applications.

1) Amino acids and peptides

1.1) Amino acids

The building blocks of proteins are mostly from 20 natural α -amino acids. Shorter length of amino acids (< 50 residues) form peptides and proteins are longer chains that take part in cell signalling and communicating processes. All α -amino acids are chiral with the exception of glycine (G) (Nelson & Cox, 2008). The structure is the same for all the common amino acids (Figure 1): a carboxyl group, an amino group, a hydrogen atom and a side chain (R group) bonded to the same carbon atom (α carbon). Amino acids differ from each other in their side chains, which vary in size, structure and electric charge. Thus, they may be classified in groups according to the nature of their side chains (polar, nonpolar, aliphatic, aromatic, neutral, positively charged and negatively charged) (Nelson & Cox, 2008). Table 1 shows the structure and properties of the 20 amino acids.

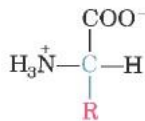
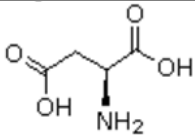
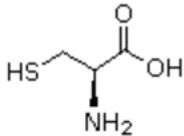
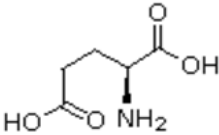
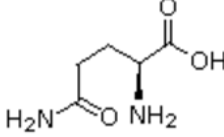
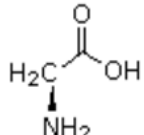
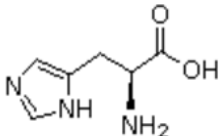
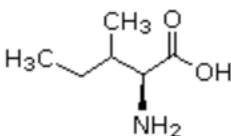
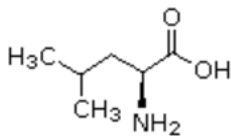
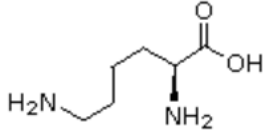


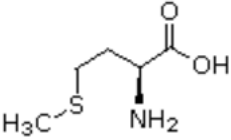
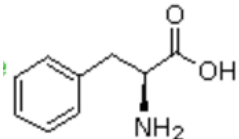
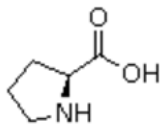
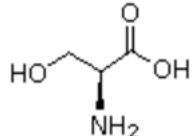
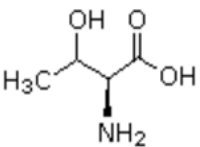
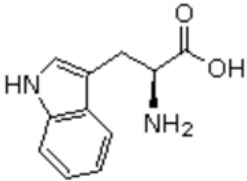
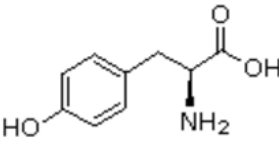
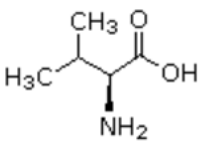
Figure 1.1- General structure of an amino acid (Nelson & Cox, 2008).

Alanine (A), valine (V), leucine (L), isoleucine (I) and methionine (M) are **aliphatic** and **nonpolar** amino acids (Nelson & Cox, 2008). The side chains of these amino acids provide a hydrophobic environment while **polar** and **neutral** amino acids (S, T, C, N, Q) are more hydrophilic because they contain functional groups (hydroxyl groups (S, T), amide groups (N, Q) or sulfhydryl group (C)) that can be involved in the formation of hydrogen bonds with water. Glycine (G) has the simplest structure compared to other amino acids due to the absence of a side chain, which makes it a flexible amino acid. On the contrary, the secondary amino group of proline (P) residues provides a reduction of the structural flexibility of polypeptides regions containing proline (Nelson & Cox, 2008). Amino acids with aromatic rings in their side chains, such as phenylalanine (F), tyrosine (Y) and tryptophan (W) belong to the **aromatic** group. These type of amino acids are hydrophobic and can interact with each other through the aromatic rings of their residues (π - π stacking). Lysine (K), arginine (R) and histidine (H) have **positively charged** (acidic) side chains at pH 7 while aspartic acid (D) and glutamic acid (E) have residues with **negative charge** (basic); both of them (either positively or negatively charged) are hydrophilic (Nelson & Cox, 2008).

Table 1.1- Structure and properties of the twenty natural amino acids. Adapted from (Mendes et al., 2013).

Amino acid	Three/One-letter code	Structure	Properties
Alanine	Ala (A)		Hydrophobic, Aliphatic, α -Helix promoting, β -sheet neutral
Arginine	Arg (R)		Hydrophilic, basic(+), α -Helix neutral, β -sheet neutral
Asparagine	Asn (N)		Polar, neutral, α -Helix breaking, β -sheet breaking

Aspartic Acid	Asp (D)		Hydrophilic, acidic (-), α -Helix neutral, β -sheet neutral
Cysteine	Cys (C)		Polar, α -Helix neutral, β -sheet promoting
Glutamic Acid	Glu (E)		Hydrophilic, acidic (-), α -Helix promoting, β - sheet breaking
Glutamine	Gln (Q)		Polar, neutral, α - Helix promoting, β -sheet promoting
Glycine	Gly (G)		α -Helix breaking, β -sheet neutral
Histidine	His (H)		Hydrophilic, basic(+), α -Helix promoting, β - sheet breaking
Isoleucine	Ile (I)		Hydrophobic, aliphatic, α -Helix neutral, β -sheet promoting
Leucine	Leu (L)		Hydrophobic, aliphatic, α -Helix promoting, β - sheet promoting
Lysine	Lys (K)		Hydrophilic, basic(+), α -Helix neutral, β -sheet breaking

Methionine	Met (M)		Hydrophobic, aliphatic, α -Helix promoting, β -sheet promoting
Phenylalanine	Phe (F)		Hydrophobic, aromatic, α -Helix promoting, β -sheet promoting
Proline	Pro (P)		α -Helix breaking, β -sheet breaking
Serine	Ser (S)		Polar, neutral, α -Helix neutral, β -sheet breaking
Threonine	Thr (T)		Polar, neutral, α -Helix neutral, β -sheet promoting
Tryptophan	Trp (W)		Hydrophobic, aromatic, α -Helix promoting, β -sheet promoting
Tyrosine	Tyr (Y)		Hydrophobic aromatic, α -Helix breaking, β -promoting
Valine	Val (V)		Hydrophobic, aliphatic, α -Helix promoting, β -sheet promoting

1.2) Peptides

A dipeptide is formed when two amino acid molecules are joined by a covalent bond called peptide bond. According to figure 1.2, the peptide bond result from the joining of the $-\text{COOH}$ group of one amino acid with the $-\text{NH}_2$ group of another. During this process, a molecule of water is eliminated (dehydration) (Nelson & Cox, 2008). Peptides may range in size from two or three to tens of linked amino acid

residues. When three amino acids are covalently linked, the product is called a tripeptide. Similarly, four peptides can be linked to form a tetrapeptide, five to form pentapeptide, and so forth (Chatterjea & Shinde, 2011). Consequently, a polypeptide is made up from many amino acids linked through peptide bonds. Proteins may consist in one or more polypeptide chains and they are present in the human body with different specific functions. Those consisting of a single polypeptide chain are considered at three structure levels: primary, secondary and tertiary structure. There is a quaternary level of structure for proteins with two or more polypeptide chains. The sequence of amino acids is the primary structure which is maintained by covalent bonds while secondary, tertiary and quaternary structures are maintained principally by noncovalent interactions (Ha & Bhagavan, 2011). All the structures are represented in figure 1.3.

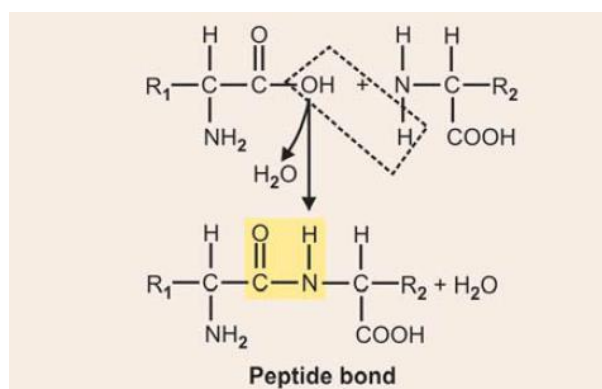


Figure 1.2- Formation of a peptide bond (Chatterjea & Shinde, 2011).

Primary structure

Primary structure corresponds to the linear sequence of amino acids linked together by peptide bonds. The primary structure dictates the properties of a protein. Thus, any change in the sequence of amino acids may affect and deregulate the properties and functions of a protein (Chatterjea & Shinde, 2011). In a peptide, the amino acid residue at the end with a free -NH_2 is the N-terminal and the free -COOH at the other end is called as C-terminal. Consequently, in a polypeptide chain the amino acids are traditionally numbered from N-terminal as number 1 towards the C-terminal (Chatterjea & Shinde, 2011).

Secondary structure

Once the primary structure is defined, the polypeptide chains can interact by hydrogen bonds between amino acids located near each other. The most common types of secondary structures are α -helix and β -sheet. A protein may have predominantly one kind of secondary structure, such as α -keratin of hair and silk fibroin containing mostly α -helix and β -sheet, respectively, or more than one kind, like haemoglobin has both α -helical and non-hydrogen-bonded regions (Ha & Bhagavan, 2011). The **α -helix** conformation is stabilised by intramolecular hydrogen bonds between carbonyl of one residue and amine of fourth amino acid residue earlier in the heptad repeat. However, the hydrogen bonding in **β -sheet** conformation is intermolecular; thus formed when a carbonyl group in the backbone of one strand bind

to the amine group from the backbone of the opposed strand; the structure is slightly pleated due to the angles of bonds and the adjacent chains are either parallel or antiparallel, depending on the arrangement between carbonyl and amine group runs in the same or opposite direction (Chatterjea & Shinde, 2011). Lastly, when a protein does not show any defined secondary structure, a **random coil** conformation is observed. In that case, the residues of the peptide chain are oriented randomly while still being bonded to adjacent units (L. J. Smith et al., 1996).

Tertiary structure

A three-dimensional structure is formed when a polypeptide chain with secondary structure is folded within itself; thus this structure is established by the steric relationship between the amino acids located far apart but brought closer by folding. Tertiary structure is maintained by hydrophobic interactions, hydrogen bonds, ionic or electrostatic interactions, van der Waals forces and disulphide bonds (Chatterjea & Shinde, 2011).

Quaternary structure

A quaternary structure exists when two or more peptide chains of the same protein (oligomer) are held together by noncovalent interactions. The hemoglobins, allosteric enzymes responsible for the regulation of the metabolism and contractile proteins (such as actin and tubulin) are examples of oligomeric proteins (Chatterjea & Shinde, 2011).

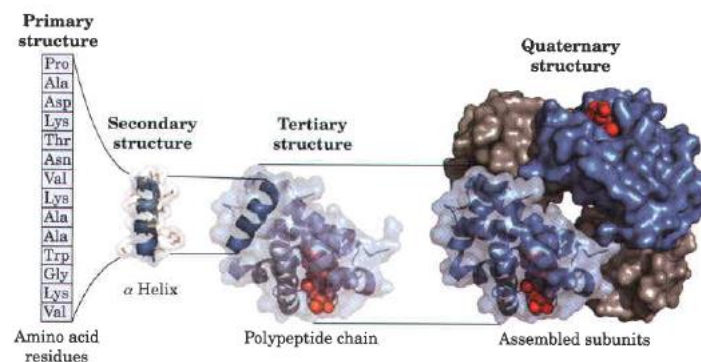


Figure 1.3- Levels of structures in proteins (Nelson & Cox, 2008).

1.3) Peptide synthesis

The need of synthetic peptides for biological applications is increasing due to the difficulty in obtaining peptides from natural sources. Thus, peptides can be obtained either through genetic engineering or chemical synthesis. Belonging to synthetic methods, solid phase peptide synthesis (SPPS) is the most used method (Mendes et al., 2013). The SPPS was first developed by Bruce Merrifield, who was awarded the Nobel Prize in 1984. This advanced technique made it practical to synthesize larger and more complex peptides with more controlled step-by-step synthesis;

consequently, the availability of synthetic peptides has revolutionized research in many biomedical areas (Coin et al., 2007).

The solid phase technique is based on growing the peptide chain on an insoluble polymeric support (resin) stepwise. During this process, the amine group and the reactive side chain of the amino acids are protected with protecting groups in order to control the reaction through the target sites and to ensure that amino acids attached to each other in a correct sequence, which are added stepwise in the C→N (from C-terminal to N-terminal) direction (Barany et al., 1987); there are diverse protecting groups that are used in SPPS, but the fluorenylmethoxycarbonyl (Fmoc) and tert-butyloxycarbonyl (Boc) are the commonly used ones.

The synthesis starts when the C-terminal of the first amino acid attaches to the resin. Once the amino acid is attached, the product is washed to remove the excess reagents and byproducts. Next, the N-terminal protecting group (Fmoc) of the attached amino acid is deprotected, leaving the N-terminal free to react with the C-terminal of the next amino acid. After 2-3 hours, the second amino acid should be coupled and the resin-peptide is washed and deprotected again, which leaves this complex ready for the next coupling cycle. Addition cycles are done until the peptide sequence is complete. Final step of synthesis is the cleavage of the peptide from the solid support and removing the protecting groups from the side chains (Barany et al., 1987).

Solid phase synthesis has provided the opportunity of designing peptide sequences and study the effect of the residues on the molecular structure of peptides; thus, it is possible to obtain a variety of nanostructures by controlling the peptide sequence.

2) Molecular self-assembly

2.1) Molecular self-assembly and supramolecular interactions

Protein's tertiary or quaternary structure, DNA double helix, cell membranes and many other biological nanostructures are formed by the process of self-assembly (Mandal et al., 2014). This process is of central importance and generates much of the functionality of the living cells. Thus, molecular self-assembly is the spontaneous organization of molecules without external control; it uses biomolecular building blocks of precisely defined shape, size, hydrophobicity, and spatial distribution (Mendes et al., 2013). A relevant example of self-assembly in nature is the double-stranded (ds) DNA molecule. Consisting of a 5-carbon sugar (deoxyribose), a nitrogen containing base attached to the sugar and a phosphate group, nucleotides are the DNA building blocks and they can be found in four different types: adenine (A), cytosine (C), guanine (G), and thymine (T); differing from each other in the nitrogenous base (Mendes et al., 2013). The alternating sugar-phosphate sequence where A, G, C and T bases extended away from the chain and stacked on the top each other, define the DNA backbone. Therefore, a double helix is formed when the complementary pairs of nucleobases (A-T and C-G) from two antiparallel strands wrapped around one another (Mendes et al., 2013). Stable hydrogen bonds are formed to sustain the strands together and reinforced by π - π stacking interactions between cyclic purine (A and G) and pyrimidine (C and T) bases. The way that these two pairs of nucleobases interact,

contributing for the stability of the DNA, defines the effectiveness of DNA replication, transcription, and ribosomal translation (Mendes et al., 2013).

According to several authors, there are two main classes of self-assembly: static and dynamic (Bishop et al., 2008; Grzybowski et al., 2009). In static self-assembly, components form ordered structures which do not change with time without energy exchange with the environment. In contrast, dynamic self-assembly corresponds to ordered nonequilibrium structures, where there is an input of energy from an external source which maintains the structures far from equilibrium (Mendes et al., 2013). The process of self-assembly is driven by attractive/repulsive forces within and between molecules. These molecules may be the same or different and the interactions between them are from the noncovalent interactions (supramolecular interactions); starting from a less ordered state leading to a final state that is more ordered (Mendes et al., 2013). Belonging to the supramolecular interactions group, the electrostatic interactions, hydrophobic effects, hydrogen bonding and aromatic stacking (π - π stacking) are the most relevant in molecular self-assembly. The hydrophobic effect is the tendency of nonpolar substances to aggregate in aqueous solution, while hydrogen bonding is the electrostatic attraction between an electronegative atom and a hydrogen atom attached to some other nearby electronegative atom. (Mendes et al., 2013). Electrostatic interactions and aromatic stacking are the most relevant interactions for this project.

Aromatic stacking correspond to attractive nonbonded interaction between planar aromatic rings. The interactions associated with the formation of these ordered stacking structures have a fundamental role in self-assembly processes leading to the formation of supramolecular structures (Claessens & Stoddart, 1997); the aromatic stacking stabilize the double-helix structures of DNA involved in core packing, the tertiary structure of proteins, host-guest interactions and porphyrin aggregation in solution (Claessens & Stoddart, 1997; Gillard et al., 1997; McGaughey et al., 1998; Shetty et al., 1996). According to many studies, aromatic rings tend to form high-order clusters of four different types: parallel displaced (face-to-face), T-shaped (edge-to-face), parallel staggered or Herringbone (figure 1.4) (Sun & Bernstein, 1996). The parallel displaced π -stacking seems to be the major organization of π - π interactions in proteins; it was suggested by the analysis of π -stacking in a group of proteins with known structures (Gazit, 2002).

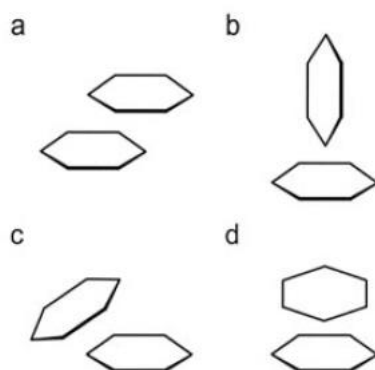


Figure 1.4- Possible π - π stacking geometries: a) parallel displaced, b) T-shape, c) parallel staggered and d) herringbone (Gazit, 2002).

Electrostatic interactions correspond to an attractive or repulsive interactions between electric charges (ion-ion interactions, dipole-dipole interaction or ion-dipole interaction). These interactions are ubiquitous in proteins and play an essential role in assembly of different building blocks, such as polyelectrolytes, charged surfactants, peptides and lipids (Mendes et al., 2013).

The characteristics of individual components (as shape, surface properties, charge, polarizability, magnetic dipole, mass, etc.) determine the way that they self-assemble with each other, through the previously described interactions. Therefore, the design of components that organize themselves into desired configurations and functions is the key for applications of self-assembly (Whitesides & Grzybowski, 2002).

2.2) Peptide self-assembly

2.2.1) Design of supramolecular materials

Supramolecular materials can be obtained by self-assembly of diverse organic and inorganic building blocks; these materials have gained much attention due to their potential applications in biology and chemistry (Whitesides et al., 1991). Among all organic building blocks, peptides are the most promising components; their biocompatibility and chemical diversity make them fascinating building blocks. Variety of structures can be obtained using 20 chemically different α -amino acids (Mandal et al., 2014). As their diversity in charge, hydrophobicity, size and polarity of their side chains provides a platform for creating different peptide sequences with distinct properties. Many important physiological and biochemical functions of life are influenced by peptides (Sacchettini & Kelly, 2002). Therefore, some human medical disorders are associated to peptides, such as the polypeptides self-assembly into amyloid fibrils in Alzheimer's disease, type II diabetes, Parkinson's diseases, among others (Glabe, 2006). Amyloid fibrils have β -sheet secondary structure generated by polypeptides of 30-40 amino acids or longer (Mandal et al., 2014). Short peptide fragments that form fibrillar structure with similar properties of amyloid fibrils, have been studied as a model system for studying amyloid fibrils formation and biological self-assembly process (Mandal et al., 2014; Reches et al., 2002).

There are several classes of self-assembling peptides, but the most common are α -helix/coiled-coil forming peptides and β -sheet forming peptides. The last one is divided into different sub-classes including self-complementary peptides, glutamine-rich peptides, β -hairpin peptides, amphiphilic peptides, multi-domain peptides and short aromatic peptides (Mendes et al., 2013). The versatility of the peptides provides a unique platform for the design of supramolecular materials. Therefore, many researchers have developed and designed novel peptide-based assemblies and investigated their possible applications in biology and nanotechnology (Mandal et al., 2014).

Ionic interactions between negatively and positively charged components within the peptides has been studied as a self-assembly mode (Caplan et al., 2000; Savin & Doyle, 2007; Zhang et al., 1993). In a study by Stupp lab, the self-assembly of peptide amphiphile (PA) molecules of opposite charges was investigated (Niece et al., 2003). They demonstrated the formation of nanofibers by electrostatic attractions when solutions of oppositely charged PAs are mixed, at neutral pH; at certain concentrations,

a 3D gel was observed. Also, Ferreira et al. demonstrated the application of electrostatic self-assembly between peptide amphiphiles. They used a microfluidic approach to drive the self-assembly into capsular structures for cell encapsulation (Ferreira, Reis, et al., 2013).

Short aromatic peptides are other class of self-assembling peptides and it was found that aromatic residues played critical roles in the process of amyloid fibrils formation (Mandal et al., 2014). Diphenylalanine (FF) is the recognition motif of the Alzheimer's β -amyloid polypeptide, leading the process of self-assembly in the molecule (Mandal et al., 2014); the dipeptide (FF) self-assemble into nanotubes through a combination of hydrogen bonding and π - π stacking of the aromatic rings (Cherny & Gazit, 2008). Different variations of these short aromatic peptides have been investigated: di- or tripeptides conjugated with bulky aromatic groups, such as fluorenylmethoxycarbonyl (Fmoc), or naphthalene, at the N-terminus (Mendes et al., 2013). Gazit et al. and Ulijin et al. have investigated the self-assembly of Fmoc-dipeptides and they showed the Fmoc protected diphenylalanine (Fmoc-FF) self-assembled into nanofibrils in aqueous solutions leading to a formation of a stable hydrogel (Gazit, 2007; Jayawarna et al., 2006; Mahler et al., 2006; Orbach et al., 2012); hydrogel characterization exhibited a biocompatible self-assembled scaffold, consisting of fibrous network (figure 1.5). In another study Ulijin et al. showed the mechanism of π - π stacking of aromatic groups and interlocked β -sheet conformation (A. M. Smith et al., 2008).

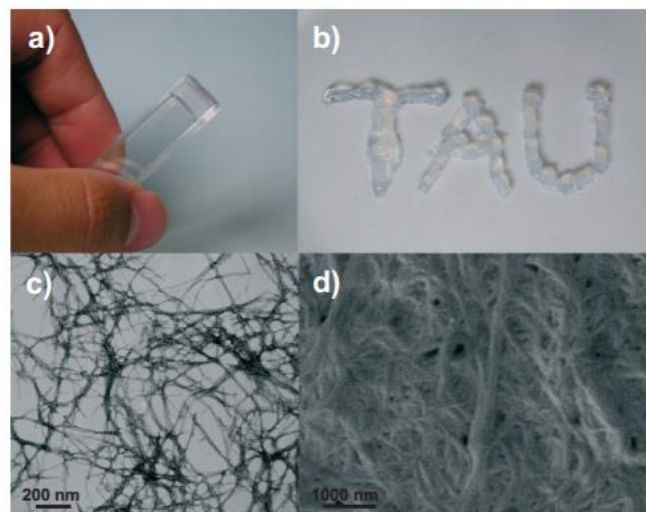


Figure 1.5- Macroscopic and microscopic analysis of the hydrogel obtained by self-assembly of the Fmoc-diphenylalanine peptide. a) The Fmoc-Phe-Phe hydrogel in the inverted cuvette; b) the letters TAU were written by injecting the gel from a syringe onto a plastic substrate; c) transmission electron microscopy image of fibrous scaffold; d) high resolution SEM image of the scaffold fibrils. Adapted from (Mahler et al., 2006).

The self-assembly of supramolecular materials can be influenced by environmental conditions such as changes in the temperature, ionic strength, concentration and pH (Mendes et al., 2013). In addition, supramolecular materials using peptides as building-blocks can be designed to co-assemble with different bio-macromolecules, such as hyaluronan (HA), to form biomaterials with interesting components for biomedical applications.

3) Hyaluronic acid

Hyaluronic acid or hyaluronan is a crucial structural component of the ECM which acts as a coordinator by concentrating and organizing the assembly of other proteins in the matrix (Jiang et al., 2011). This negatively charged polysaccharide is a nonsulfated glycosaminoglycan of repeating units of D-glucuronic acid (GlcA) and N-acetyl-D-glucosamine (GlcNAc) linked by glycosidic ($\beta(1\rightarrow3)$ and $\beta(1\rightarrow4)$) linkage (Figure 1.6) (Jiang et al., 2011).

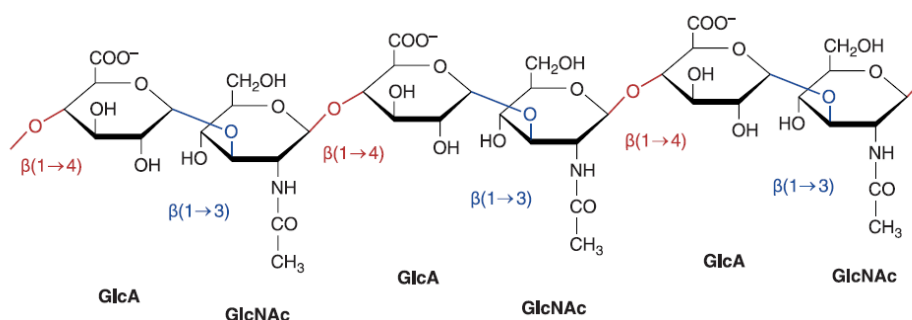


Figure 1.6- Chemical structure of hyaluronan: three repeating units for the disaccharide GlcA-GlcNAc are shown (Jiang et al., 2007).

Hyaluronan is present in a wide range of organisms, such as in simple bacteria to complex eukaryotes; where HA can be found in the vitreous of the eye, skin, skeletal tissues, umbilical cord, heart valve and synovial fluid of the human body (Jiang et al., 2011). Some of the numerous functions of hyaluronan are hydration, space filling, lubrication of joints and providing cell migration (Toole, 2004). Furthermore, this polysaccharide regulates some aspects of molecular mechanisms of tissue repair such as activation of inflammatory cells to start an immunological response and regulating the behaviour of epithelial cells (Jameson et al., 2005; Teriete et al., 2004).

Several studies have been reported on combining hyaluronan and self-assembling peptides. In 2008, Capito et al. reported the self-assembly of macroscopic sacs and membranes at the interface between two aqueous solutions of HA and a peptide amphiphile (PA) with opposite charges (Capito et al., 2008). A hierarchical self-assembly process between the hyaluronan and the PA resulted the formation of the membranes. Initially, researchers observed the formation of a dense barrier between the two liquids, preventing their chaotic mixing; then the growth of the membrane was driven by a dynamic synergy between osmotic pressure of ions and static self-assembly, leading to a formation of a membrane with a highly ordered structure (Capito et al., 2008). In a later report, Chow and co-workers developed a bioactive self-assembling membrane to promote angiogenesis, by combining the hyaluronan with a heparin-binding PA (Chow et al., 2011). These self-assembling membranes can be used as an artificial ECM, which can mimic the properties of native tissues, as well as to recreate cellular microenvironments. Ferreira et al. used self-assembling bioactive HA/PA membranes presenting biochemical signals (RGDS) as wound-healing biomaterial for skin (Ferreira, Marques, et al., 2013). The resulted membranes revealed a very highly organized structure exhibiting two distinct surfaces, one corresponding to HA side and other to peptide side (figure 1.7). HA side was characterized by a rough

and amorphous structure, while the peptide side exhibits a network of nanofibers randomly distributed, that resembles the ECM network. Furthermore, SEM analysis of the cross section revealed aligned nanofiber bundles perpendicular to the interface (Ferreira, Marques, et al., 2013).

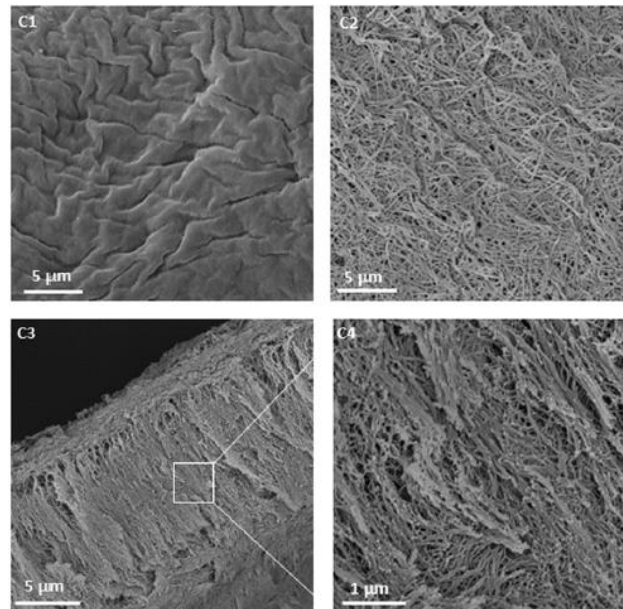


Figure 1.7- SEM images of self-assembled membranes with 1% (w/v) HA and 2% (w/v) K-PA showing the HA side (C1), peptide side (C2) and cross section (C3, C4) (Ferreira, Marques, et al., 2013).

Understanding the mechanism and functions of hyaluronan is crucial for developing novel treatments for many diseases. Thus, HA has become an important building block for the creation of new biomaterials and it can be cross-linked to a variety of proteins, in order to generate structures with different designs and functional activities with interest in tissue engineering and regenerative medicine (Burdick & Prestwich, 2011).

4) Aim

The degradation of the extracellular matrix components over time and consequently the need for tissues repair and regeneration has motivated the development of novel biomaterials and scaffolds (Holmes, 2002). Self-assembled biomaterials using peptides as building blocks have been shown as a promising solution. Once combining different amino acids, it is possible to produce a variety of structures that recreates some of architectural features of ECM. The aim of this project is to develop novel hyaluronan base hydrogels obtained by supramolecular interactions with peptides for biomedical applications.

Several peptides were designed to form supramolecular interactions with HA and induce gel formation, following π - π stacking and electrostatic interactions. The peptide design is based on ABC blocks in which A block corresponds to charged residues (lysine), B block is spacer (such as glycine chain) and C block is aromatic residues (phenylalanine). Different designs of peptide were synthesized

and gel formation was investigated. It was expected that the positive charge (lysine) of the peptides interact with the hyaluronic acid (negative charge) and the aromatic rings (phenylalanine residues) interact to each other through π - π stacking to form hydrogels.

CHAPTER 2: Materials and Methods

In this chapter the synthesis, purification and characterization of the peptides NH₂-KG₂F-CONH₂, Ac-KG₅F-CONH₂, Ac-K₂G₅F-CONH₂, Ac-KG₅F₃-CONH₂, Ac-K₃G₅F₃-CONH₂ and Ac-K₂G₇F₄-CONH₂, as well as peptides/HA hydrogels preparation and characterization are described. Also, the background information on the purification and characterization equipment were described in detail.

1) Peptide synthesis

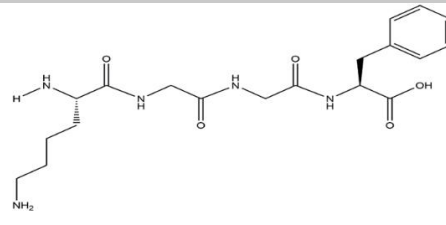
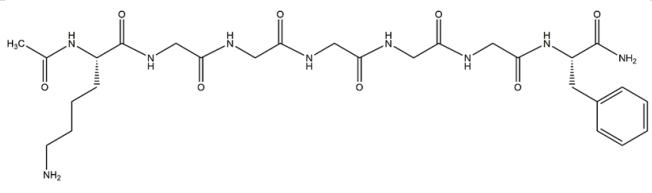
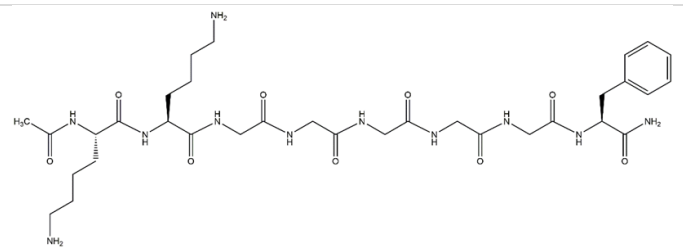
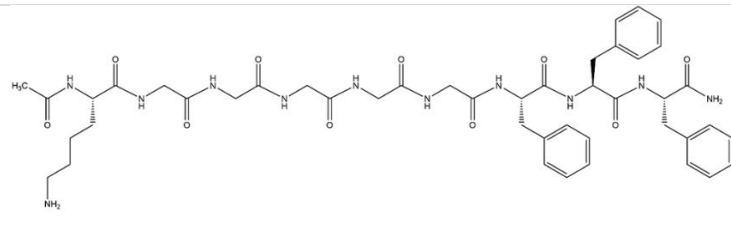
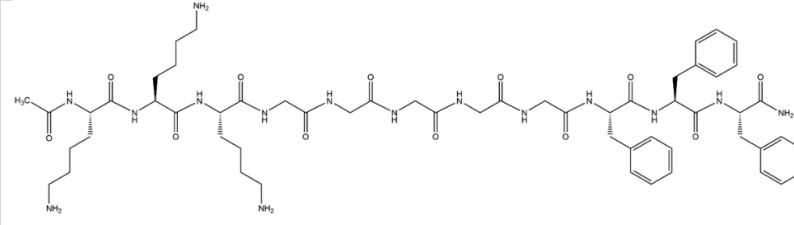
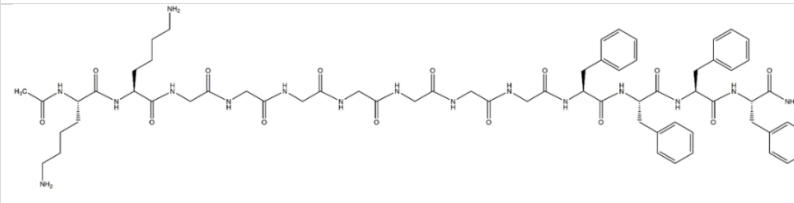
Solid-phase peptide synthesis following the Fmoc protocol are described in this section. Furthermore, the chemical structure, molecular weight and synthesis scale of the synthesized peptides are shown in table 2.1.

Materials: Fmoc-Lys(Boc)-OH, Fmoc-Gly-OH and Fmoc-Phe-OH were obtained from Novabiochem, UK. Rink amide MBHA resin obtained from Novabiochem, UK. N,N'-Diisopropylcarbodiimide, 99% (DIC, Alfa Aesar, UK); Piperidine, 99.9% (PIP, Sigma-Aldrich, UK); Triisopropylsilane, 98% (TIS, Alfa Aesar, UK); Dichloromethane (DCM, Fisher Scientific, UK); Dimethylformamide (DMF, VWR, US); 1-Hydroxybenzotriazole Hydrate (HOBT, Carbosynth, UK); Acetic Anhydride 99% (Acros Organics, USA); Trifluoroacetic acid, 99% (TFA, Sigma-Aldrich, UK); Diethyl ether (Sigma-Aldrich, UK); Acetonitrile (ACN, Sigma-Aldrich, UK); Kaiser teste from Fluka Analytical USA with three reagents: phenol solution (80% in ethanol), Potassium cyanide solution and C: Ninhydrin Solution (6% ethanol) were used as received.

Solid phase peptide synthesis

The peptides were synthesized in an automated peptide synthesizer (CEM, Liberty Blue, UK) or manually using standard 9-fluorenylmethoxycarbony based solid-phase chemistry approach and a rink amide resin (100-200 mesh) with substitution degree of 0.78 mmol/g. The calculations for each peptide were done for the scales shown in table 2.1. Amino acid couplings were performed using 4 equivalents of amino acid, 4 equivalents of HOBT and 4 equivalents of DIC. Deprotections were performed using 20% piperidine in DMF. Before the cleavage, the acetylation of the some peptide's N-terminal was carried out by using a solution preformed with 10% Acetic Anhydride in DMF. The cleavage solution (prepared with a mix of TFA/TIS/water (95%/2.5%/2.5%)) was added and mixed for 3 hours to cleave the peptides from the resin. The peptide mixtures were collected and TFA was removed by rotary evaporation. At the end, cold diethyl ether was used for precipitation and the peptides were collected using a centrifuge (Heraeus Multifuge X1, Thermo Scientific, USA) for 20 minutes with 5000 rpm at 2 °C and freeze-dried to obtain the peptides in the powder form.

Table 2.1- Peptide sequences, chemical structure, molecular weight and synthesis scale.

Peptide sequences	Chemical structure	Molecular weight (g/mol)	Synthesis scale
NH ₂ -K ₂ G ₂ F-CONH ₂		407.47	0.5 mmol
Ac-KG ₅ F-CONH ₂		619.68	0.25 mmol
Ac-K ₂ G ₅ F-CONH ₂		747.86	0.5 mmol
Ac-KG ₅ F ₃ -CONH ₂		914.03	0.25 mmol
Ac-K ₃ G ₅ F ₃ -CONH ₂		1170.38	0.25 mmol
Ac-K ₂ G ₇ F ₄ -CONH ₂		1303.49	0.5 mmol

2) Peptide Purification and Characterization

Peptides were purified by preparative High Performance Liquid Chromatography (HPLC), their masses were confirmed by Electrospray Ionization Mass Spectrometry (ESI-MS) and their purity was analysed by analytical HPLC. Furthermore, Circular Dichroism (CD) spectroscopy was used to examine the secondary structure of the peptides.

Materials: Acetonitrile (ACN, Sigma-Aldrich, UK) and Trifluoroacetic acid, 99% (TFA, Sigma-Aldrich, UK) were used as mobile phase for the HPLC. Methanol (Sigma-Aldrich, UK) and Formic acid (Sigma-Aldrich, UK) were used as received.

2.1) ESI-MS

Mass spectrometry is a characterization technique for evaluating the molecular masses of different components by fragmenting them into ions and then measuring the response of their trajectories to electric and magnetic fields or both (Whitehouse et al., 1989). The mass spectrometry analysis consists essentially of three steps. The first step corresponds to the ionization process that converts the molecules or atoms into gas-phase ionic species. After ionization, the molecular ions and their charged fragments are separated by a mass analyser based on their m/z (mass-to-charge) ratios (second step); the direction of the components is controlled by magnetic or electric fields. Finally, the generated ion current is measured, amplified, and displayed as a mass/charge spectrum (Dass, 2007; R. D. Smith et al., 1991). The spectrum is m/z versus the signal intensity. The most abundant ion in the spectrum is generally designated as the base peak and the peaks of all other ions are reported as percentage abundances relative to this base peak. In order to better understand the data, it is essential to know the theoretical molecular weight of the compound and its possible molecular ions, which are obtained as protonated or deprotonated molecule ($[M+H]^+$ or $[M-H]^-$) depending on the sample characteristics (Dass, 2007).

Furthermore, it is important to note that the first two steps are carried out under vacuum to allow the free movements of the ions in space, preventing them from colliding or interacting with other species (Dass, 2007). Relatively to the ionization process of the first step, there are various types of ionization methods, such as electron impact (EI), fast atom bombardment (FAB), photoionization (PI) and electrospray ionization (ESI) (Dass, 2007). Additionally, the mass analyser mentioned in the second step exists in different types and the most common are fourier transform ion cyclotron resonance, time of flight, orbitrap and linear quadrupole ion, quadrupole mass filter and three-dimensional quadrupole ion trap (Dass, 2007); A single quadrupole (SQ) mass analyser was used in this work and the others will not be described here. The quadrupole mass analyser consists of four parallel rods that generate a radio frequency quadrupole field between them (Dawson, 2013). The oscillation and the variation of the potential of the rods allows for the control of the direction of the ions and acts as a filter that permits an ion of a certain mass-to-charge ratio to pass through it while rejecting all others (Dawson, 2013).

Mass detection was performed by SQ detector 2 (Waters, UK) with a mass range up to 3000 Da, and the data were processed in MassLynx® software. The sample was prepared as 0.1 mg/ml concentration of peptides dissolved in water methanol mixture and filtered through 0.2 µm membrane before MS analysis.

2.2) HPLC

HPLC is a powerful technique used for the separation of different components such as proteins, which takes advantage of differences in protein charge, size, binding affinity, and other properties (Nelson & Cox, 2008). Thus, chromatographic separation is based on differences in the rates of migration of the sample components through a column (Engelhardt, 2012). Depending on the type of chromatographic technique, different columns are used, but these techniques consist of a porous solid material with appropriate chemical properties (the stationary phase) and a buffered solution (the mobile phase) (Nelson & Cox, 2008). Depending on their properties, the molecules on the mobile phase migrate faster or slower through the column. The mobile phase can be either a gas or a liquid and several types of HPLC may be identified; classification is based on the type of mobile and stationary phase used (Engelhardt, 2012). In this work, reversed phase high performance liquid chromatography (RP-HPLC) was performed.

RP-HPLC separate the components of the sample based on the hydrophobicity of the sample; the separation depends on the hydrophobic binding between molecules from the mobile phase and the immobilized hydrophobic ligands attached to the stationary phase (Aguilar, 2004). Since each component in the sample interacts differently with the stationary phase, different retention times can be observed. Therefore, polar components have lower retention times as compared to molecules with less polarity, which take longer time to elute. RP-HPLC usually contains an silica based stationary phase, that is surrounded by covalently bonded functional groups such as C18, from which the mobile phase are eluted with gradients of increasing concentrations of organic solvents such as ACN containing an ionic modifier like TFA (Aguilar & Hearn, 1996; Mant & Hodges, 1996). Furthermore, preparative HPLC system is used when the main objective is peptide purification; which is similar to the analytical system but has a mass detector associated to it.

Before purification, the analytical HPLC (Alliance HPLC System, Waters, UK) with X-bridge column (C18, 3.5 µm, 4.6 x 150 mm) was used to analyse the purity of the peptides (1 mg/ml) and also to obtain information about the elution times in order to optimize the eluent gradient for preparative HPLC. The UV detector was set at 220 nm for the detection of the peptide bonds and Empower® software was used for data acquisition and processing. The peptides were purified in a preparative HPLC (Waters 2545 Binary Gradient HPLC system, Waters, UK) containing reverse-phase C18 column (X-bridge Prep OBD, 5 µm, 30 x 150 mm, Waters, UK). Peptides were eluted using a gradient of 0.1% TFA/water and 0.1% TFA/ACN. After the purification process, the solvent was removed by rotary evaporation followed by freeze-drying to obtain the peptides in the powder form. The gradient used for analysing the peptides is shown in table 2.2.

Table 2.2- Gradient used for analysing the peptides

Time (min)	0.1% TFA/H ₂ O	0.1% TFA/ACN
2	98	2
42	0	100

2.3) CD spectroscopy

Circular dichroism (CD) is a technique that has been used to analyse the secondary structure of proteins, polypeptides and peptides (Whitmore & Wallace, 2008). CD refers to the differential absorption of the left and right circularly polarised components of plane-polarised radiation; observed when a chromophore is chiral (optically active) (Kelly & Price, 2000). In practice, the analysis starts when a modulator subjected to an alternating electric field splits the radiation into its two circularly polarised components and then it passes through the sample (Kelly & Price, 2000). If the left and right circularly polarised components are not absorbed or are absorbed to the same extent, the combination of the components would generate radiation polarised in the original plane. However, if one of the components is absorbed in a different extent than the other, the resulting radiation would be elliptically polarised (Kelly & Price, 2000). Actually, the CD instrument does not recombine the two components, but detects it separately; it then shows the dichroism at a given wavelength of radiation expressed as either the difference in absorbance of the two components or as the ellipticity in degrees (Kelly & Price, 2000). CD signals are only observed where absorption of the radiation occurs, and thus spectral bands, corresponding to distinct structural properties of a molecule, are observed (Kelly et al., 2005). The interesting chromophores for analysing the secondary structure of proteins include the peptide bond, aromatic amino acid chains and disulphide bonds. Peptide bond (absorption below 240 nm) is the principal absorbing group for the study of the secondary structure. Thus, proteins exhibiting different types of secondary structure give rise to characteristic CD spectra in the far UV (Kelly et al., 2005). Furthermore, reference spectra derived from proteins of known structure have been developed as a support and reference for interpretation of the CD spectra of novel peptides.

The secondary structure of the peptides was analysed with circular dichroism (CD) spectroscopy using a Pistar-180 spectrometer from Applied Photophysics (Surrey, UK) under a constant flow of nitrogen (8 L/min) at a constant pressure value of a 0.7 MPa. The measurements were recorded at 25 °C from 190 to 300 nm far-UV spectra. The samples were prepared in deionized water with concentrations and pHs according to the table 2.3. All samples were tested in a quartz cuvette with 1 mm path-length and all scans were performed in the steady state with a bandwidth.

Table 2.3- Peptide solutions for CD analysis: concentration and pH.

Sequence	Concentration	pH
NH ₂ -KG ₂ F-CONH ₂	0.01 mM	7, 11
Ac-KG ₅ F-CONH ₂	0.1 mM, 0.05 mM	4, 7, 10
Ac-K ₂ G ₅ F-CONH ₂	0.1 mM	2, 4.7, 10
Ac-KG ₅ F ₃ -CONH ₂	0.1 mM	2, 7, 10
Ac-K ₃ G ₅ F ₃ -CONH ₂	0.01 mM	3, 7, 10
Ac-K ₂ G ₇ F ₄ -CONH ₂	0,01 mM	4, 8, 10

3) Peptide-HA hydrogels preparation

In order to obtain hydrogels, the peptides were combined with HA with different molecular weights. In this point, the diverse combinations that were tested for each synthesized peptide are described. Furthermore, it is important to refer that the investigation of gel formation of the Ac-K₂G₅F-CONH₂ (P3) peptide are described before of the Ac-KG₅F-CONH₂ (P2), once the P3 was ready from the purification process earlier than the peptide that was synthesized before (P2).

Materials: Hyaluronic Acid 700 kDa, 200 kDa, 60 kDa, 20 kDa and 5 kDa were used as received from Lifecore Biomedical, Inc. (Chaska, USA).

▪ NH₂-KG₂F-CONH₂ (P1)

The peptide was dissolved in ultrapure water (2% w/v) and combined with 2% (w/v) HA solutions of different molecular weights (200, 60 and 5 kDa) in two 96-well plate, as represented in table 2.4. First, the HA solution was injected into a well and then the peptide solution was added over HA, with the exception of the last line of the table 2.4 whereby the peptide solution was injected inside the HA solution. One of the 96-well plate was left at 60°C in a water bath and the other at room temperature.

Table 2.4- Gel formation investigation for peptide NH₂-KG₂F-CONH₂.

200 kDa HA	60 kDa HA	5 kDa HA
60 µl HA + 60 µl P1	60 µl HA + 60 µl P1	60 µl HA + 60 µl P1
60 µl HA + 120 µl P1	60 µl HA + 120 µl P1	60 µl HA + 120 µl P1
60 µl HA + 120 µl P1 + 60 µl HA	60 µl HA + 120 µl P1 + 60 µl HA	60 µl HA + 120 µl P1 + 60 µl HA
60 µl HA + 120 µl P1 (injected inside)	60 µl HA + 120 µl P1 (injected inside)	60 µl HA + 120 µl P1 (injected inside)

▪ Ac-K₂G₅F-CONH₂ (P3)

In order to teste the effect of different ionic states of the lysine on the formation of self-assembled nanostructures, two peptide solutions (2% w/v) with different pH (normal and acid) were combined with 2% (w/v) HA solutions of different molecular weights. All the combinations are exhibited in table 2.5.

Table 2.5- Gel formation investigation for peptide Ac-K₂G₅F-CONH₂.

700 kDa HA	200 kDa HA	60 kDa HA	5 kDa HA
	60 µl HA + 60 µl P3	60 µl HA + 60 µl P3	
60 µl HA + 60 µl P3 + 60 µl HA	60 µl HA + 60 µl P3 + 60 µl HA	60 µl HA + 60 µl P3 + 60 µl HA	60 µl HA + 60 µl P3 + 60 µl HA
60 µl HA + 120 µl P3	60 µl HA + 120 µl P3	60 µl HA + 120 µl P3	60 µl HA + 120 µl P3
60 µl HA + 120 µl P3 + 60 µl HA	60 µl HA + 120 µl P3 + 60 µl HA	60 µl HA + 120 µl P3 + 60 µl HA	60 µl HA + 120 µl P3 + 60 µl HA
60 µl HA + 60 µl P3 (pH= 3)	60 µl HA + 60 µl P3 (pH= 3)	60 µl HA + 60 µl P3 (pH= 3)	60 µl HA + 60 µl P3 (pH= 3)

In the previous tests (table 2.4 and 2.5) no gel formation was observed, as will be described in chapter 3. Thus, new strategies for combining the peptide with HA were adopted such as increasing the concentration of the peptides and HA, increasing the temperature, mixing the peptide in powder form with HA, among others.

The peptide Ac-K₂G₅F-CONH₂ was dissolved in water (10% w/v) and was incubated at room temperature. Also, 30 µl of this peptide solution was combined 2% (w/v) HA. Figure 2.1 shows all this process. Moreover, the peptide in the powder form was combined with 2% (w/v) HA solutions of different molecular weights, according to table 2.6.

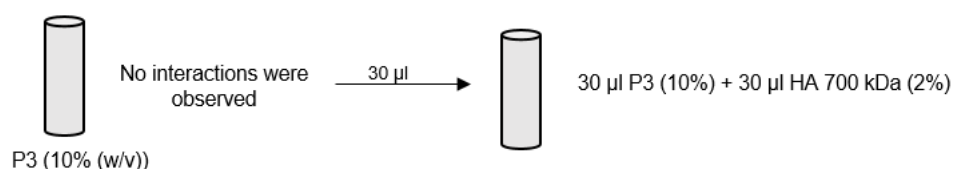


Figure 2.1- Gel formation investigation for peptide Ac-K₂G₅F-CONH₂ with 10% (w/v).

Table 2.6- Gel formation investigation for peptide Ac-K₂G₅F-CONH₂ in powder form.

700 kDa HA	200 kDa HA	60 kDa HA	20 kDa
0.005 g P3 (powder) + 50 µl HA	0.005 g P3 (powder) + 50 µl HA	0.005 g P3 (powder) + 50 µl HA	0.005 g P3 (powder) + 50 µl HA

▪ **Ac-KG₅F-CONH₂ (P2)**

The peptide was dissolved in water (10% w/v) and incubated at room temperature. Then, 20 µL of peptide solution was combined with 60 kDa 2% (w/v) HA solution. This process is represented in the following figure.

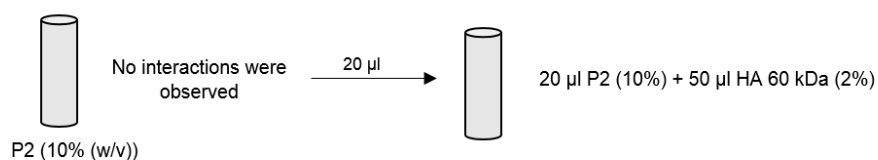


Figure 2.2 - Gel formation investigation for the peptide Ac-KG₅F-CONH₂.

Furthermore, the peptide in the powder form was combined with 2% (w/v) HA solutions of different molecular weights (700, 200, 60 and 20 kDa), according with the table 2.7.

Table 2.7- Gel formation investigation for the peptide Ac-KG₅F-CONH₂ in powder form.

700 kDa HA	200 kDa HA	60 kDa HA	20 kDa
0.005 g P2 (powder) + 50 µl HA	0.005 g P2 (powder) + 50 µl HA	0.005 g P2 (powder) + 50 µl HA	0.005 g P2 (powder) + 50 µl HA

▪ **Ac-KG₅F₃-CONH₂ (P4)**

According to figure 2.3, 10% and 20% (w/v) peptide solutions were incubated at room temperature. After 24 hours, no gel formation was observed for the two peptides solutions. So, the 10% peptide solution was divided and 2% HA solutions with different molecular weights were added. The 20% peptide solution was incubated at 60 °C.

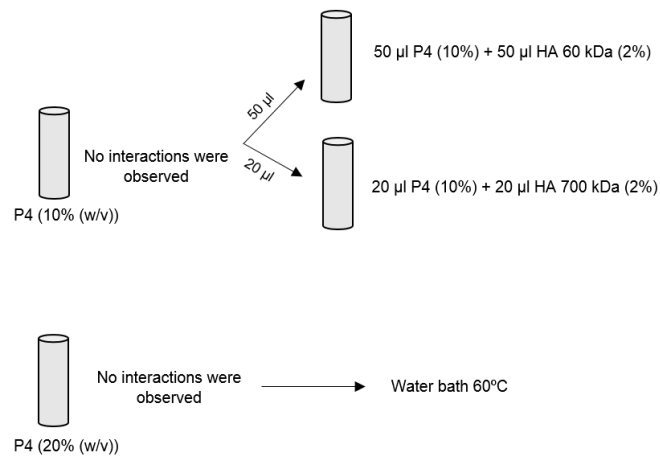


Figure 2.3 - Gel formation investigation for peptide Ac-KG₅F₃-CONH₂.

For this peptide, the gel formation using the peptide in powder form was also investigated. However, besides 2% (w/v) HA solutions that has been used before, 1% were tested too. All the combinations are shown in table 2.8. The samples were incubated at room temperature and 60 °C for 24 hours.

Table 2.8- Gel formation investigation for peptide Ac-KG₅F₃-CONH₂ in powder form.

700 kDa HA	200 kDa HA	60 kDa HA	20 kDa
0.005 g P4 (powder) + 100 µl HA (2%)	0.005g P4 (powder) + 100 µl HA (2%)	0.005g P4 (powder) form + 100 µl HA (2%)	0.005 g P4 (powder) + 100 µl HA (2%)
0.005g P4 (powder) + 100 µl HA (1%)	0.005g P4 (powder) + 100 µl HA (1%)	0.005g P4 (powder) + 100 µl HA (1%)	0.005g P4 (powder) + 100 µl HA (1%)

▪ Ac-K₃G₅F₃-CONH₂ (P5)

As it was done before for the other peptides, the gel formation between 10% (w/v) peptide solution combined with 2% (w/v) HA solution was investigated (figure 2.4); as well as, the peptide in powder form combined with 2% HA with different molecular weights (table 2.9).

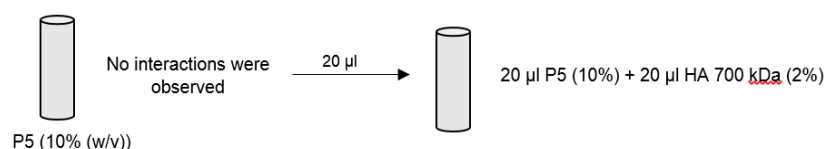


Figure 2.4- Gel formation investigation for peptide Ac-K₃G₅F₃-CONH₂.

Table 2.9- Gel formation investigation for peptide Ac-K₃G₅F₃-CONH₂ in powder form.

700 kDa HA	200 kDa HA	60 kDa HA	20 kDa
0.005 g P5 (powder) + 100 µl HA	0.005 g P5 powder form + 100 µl HA	0.005 g P5 (powder) + 100 µl HA	0.005 g P5 (powder) + 100 µl HA
0.01 g P4 (powder) + 80 µl HA	/	/	/

▪ **Ac-K₂G₇F₄-CONH₂ (P6)**

For the last gel formation investigation, was only used the peptide in powder form. It was combined with ultrapure water and 2% (w/v) HA solutions of different molecular weights, according with table 2.10. After one day of gel formation investigation at room temperature, the solutions were incubated at 60 °C.

Table 2.10- Gel formation investigation for the peptide Ac-K₂G₇F₄-CONH₂ in powder form.

700 kDa HA	200 kDa HA	60 kDa HA	20 kDa	H ₂ O
0.005 g P6 (powder) + 100 µl HA	0.005 g P6 (powder) + 100 µl HA	0.005 g P6 (powder) + 100 µl HA	0.005 g P6 (powder) + 1000 µl HA	0.005 g P6 (powder) + 25 µl H ₂ O (20%)

4) Peptide-HA hydrogels characterization

4.1) SEM

Materials: Phosphate buffered saline (PBS, Sigma) was obtained in tablets and each tablet was diluted in 200 ml water and the pH was checked to be at 7.4. Glutaraldehyde (25%, MERCK) was diluted in PBS (×10 times).

Scanning electron microscopy is an imaging technique that allows the examination and analysis of the microstructural characteristics of the materials (Zhou & Wang, 2007). The imaging principle is through the acceleration of electron beams via electromagnetic or electrostatic lens and the reflection of these beams with the material surface (Egerton, 2006). A beam of electrons (primary electrons) are focused into a small-diameter electron probe that is scanned across the specimen; electromagnetic or electrostatic fields are used to accelerate the electrons. Then, by scanning simultaneously in two perpendicular directions, an area of specimen can be covered and an image is formed by collecting the reflected or secondary electrons from each point on the specimen (Egerton, 2006).

Inspect F scanning electron microscope (Oxford instruments) was used to analyze the microstructure of the gels. Since the scanning takes place under the vacuum, the samples should be dried and conductive. For this reason, 2.5% glutaraldehyde in PBS solution was prepared for the fixation of the samples, where the samples were immersed in the solution and then they were left overnight in the fridge. Before dehydration, the samples were washed three times with PBS. Dehydration of samples was performed in ethanol solutions with increasing concentrations (20, 50, 60, 80, 90, 95 and 100%) and the samples were left in each solution for 15 minutes and overnight in 100% ethanol. Then the samples were dried by using critical point dryer (EMS 850 Quorum). In order to make the samples conductive, they were coated with gold for 30 seconds.

CHAPTER 3: Results and Discussion

In this chapter, the results of peptide synthesis and purification as well as hydrogels preparation and characterization are presented and discussed.

1) Peptide synthesis

The peptides were successfully synthesised by the Fmoc protocol and the details (mass after purification, yield and solubility) are shown in table 3.1. The yield was calculated based on the theoretical molecular weight of each peptide (shown on table 2.1) and the actual mass recovered after purification; only the yield calculations for the first peptide are demonstrated here, the calculations for the remaining peptides are shown in appendix 1.

Table 3.1- Solubility, mass after purification and yield of the synthesised peptides.

Peptides	Solubility	Mass after purification (gr)	Yield (%)
NH ₂ -KG ₂ F-CONH ₂	Soluble in water	0.1831	89.9
Ac-KG ₅ F-CONH ₂	Soluble in water	0.1242	80.2
Ac-K ₂ G ₅ F-CONH ₂	Soluble in water	0.3601	96.3
Ac-KG ₅ F ₃ -CONH ₂	Soluble in water	0.1934	84.6
Ac-K ₃ G ₅ F ₃ -CONH ₂	Soluble in water	0.1962	67.1
Ac-K ₂ G ₇ F ₄ -CONH ₂	Soluble in water	0.6241	95.8

The first peptide (NH₂-KG₂F-CONH₂) was synthesised in 0.5 mmol scale and its theoretical molecular weight is 407.47 g/mol. Thus, the expected mass for the synthesised peptide would be 0.2037 g, according with the following equation.

$$\frac{0.5}{1000} \text{ mol} \times 407.47 \frac{\text{g}}{\text{mol}} = 0.2037 \text{ g} \quad (3.1.1)$$

After purification, a mass of 0.1831 g was obtained and consequently the obtained yield was 89.9%.

$$\text{yel} (\%) = \frac{0.1831 \text{ g}}{0.2037 \text{ g}} \times 100\% = 89.9\% \quad (3.1.2)$$

All peptides were obtained with good yields, with exception of the Ac-K₃G₅F₃-CONH₂. This can be related with some errors that may occur during the synthesis procedures. Furthermore, all the peptides were soluble in ultrapure water, making easier the preparation of the samples for the purification and characterization techniques.

2) Peptide purification and characterization

The molecular masses of the synthesised peptides were confirmed by ESI-MS, their purity by HPLC and their secondary structure by CD. The results and discussion of this techniques are described in this point.

2.1) ESI-MS

As mentioned before in chapter 2, the highest intensity peak in the m/z spectrum is generally designated as the base peak, corresponding to the most abundant ion, and the remaining peaks are related to the other possible ionizable states. Therefore, it is essential to know the theoretical molecular weight of the peptide and its possible molecular ions, which are obtained as protonated molecule ($[M + H]^+$), to interpret the MS spectra. Thus, the possible m/z (ratio of molecular mass to the number of charges) values can be expressed as follows:

$$m/z = \frac{[Mw + nH^+]}{n} \quad (3.2.1)$$

Where, Mw represents the molecular mass of the peptide, n the number of charges and H is the mass of a proton (1.008 Da). Through this equation, the possible peaks of the molecular ions for each synthesised peptide were calculated and listed in table 3.2. In the present work, the possible ionizable states of the synthesised peptides are defined by the number of lysines that are present on it, once lysine is the only charged amino acid of the sequence.

Table 3.2- Possible m/z of the synthesised peptides.

Peptide	m/z
$\text{NH}_2\text{-KG}_2\text{F-CONH}_2$	$[M + H^+] = 408.57$
$\text{Ac-KG}_5\text{F-CONH}_2$	$[M + H^+] = 620.68$
$\text{Ac-K}_2\text{G}_5\text{F-CONH}_2$	$[M + H^+] = 748.86$ $\frac{[M + 2H^+]}{2} = 374.93$
$\text{Ac-KG}_5\text{F}_3\text{-CONH}_2$	$[M + H^+] = 915.03$
$\text{Ac-K}_3\text{G}_5\text{F}_3\text{-CONH}_2$	$[M + H^+] = 1171.38$ $\frac{[M + 2H^+]}{2} = 586.19$ $\frac{[M + 3H^+]}{3} = 391.13$
$\text{Ac-K}_2\text{G}_7\text{F}_4\text{-CONH}_2$	$[M + H^+] = 1304.49$ $\frac{[M + 2H^+]}{2} = 652.75$

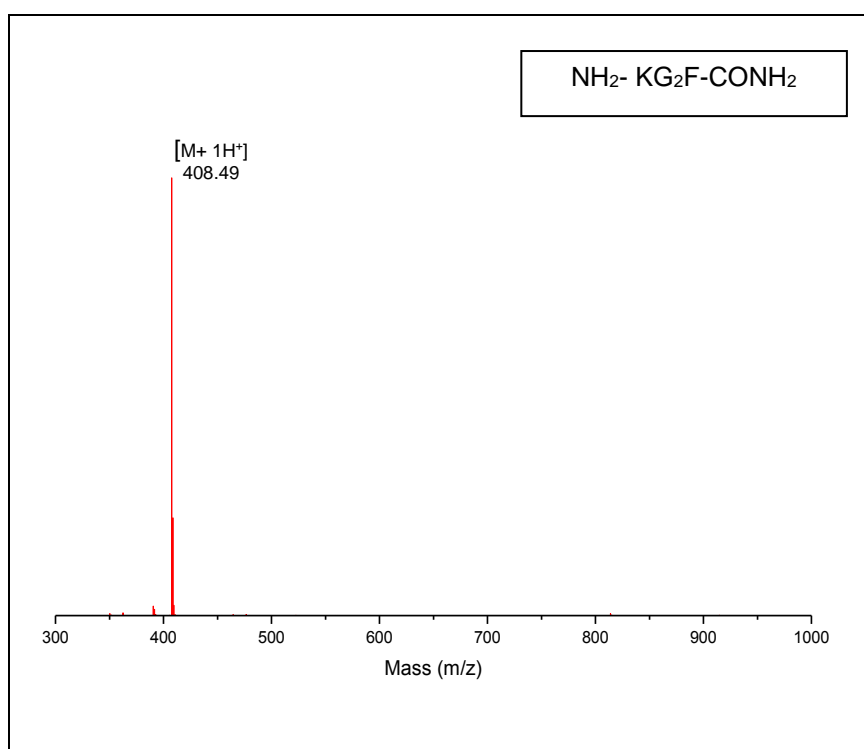
The MS results of the synthesised peptides are shown on figure 3.1.

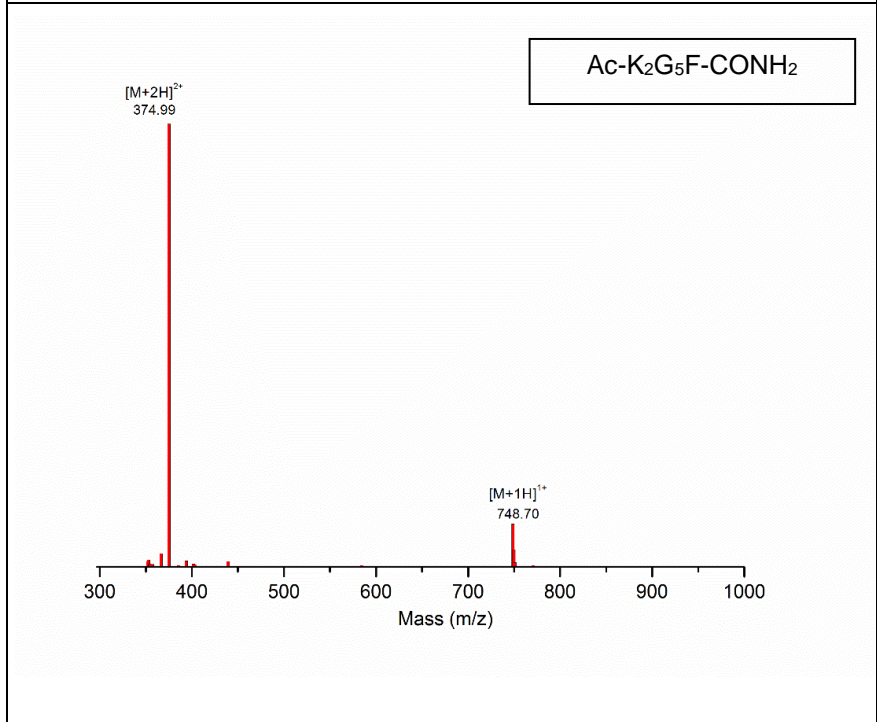
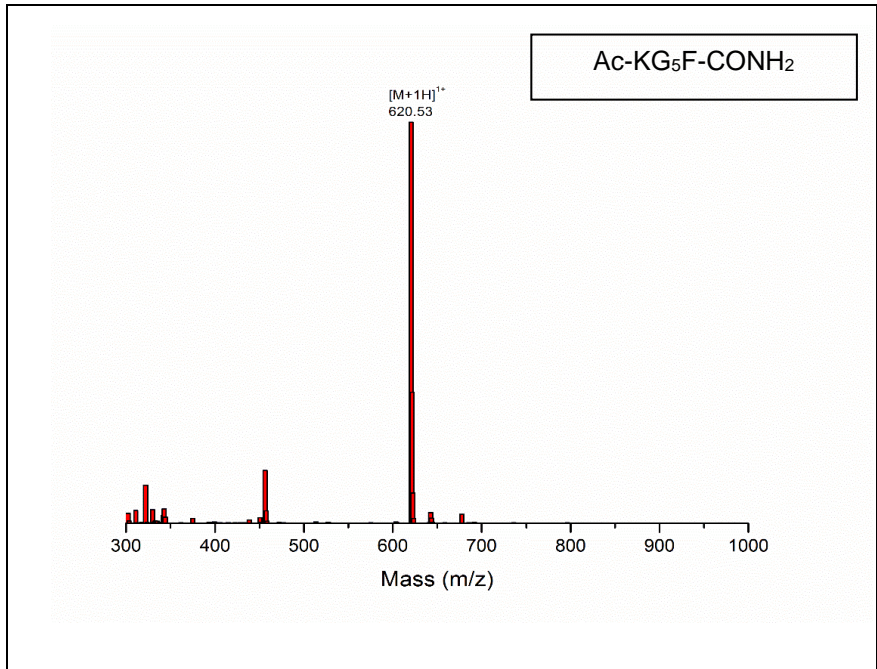
Through the analysis of the $\text{NH}_2\text{-KG}_2\text{F-CONH}_2$, $\text{Ac-KG}_5\text{F-CONH}_2$ and $\text{Ac-KG}_5\text{F}_3\text{-CONH}_2$ m/z spectra, it is possible to identify, respectively, one major peak of $[\text{M}+\text{H}]^+$ that is related to the ionization states of the each peptide: 408.49, 620.53 and 914.78 m/z. Since each peptide has only one lysine in its sequence, only one ionic species can be reported on the MS spectrum. Although other peaks that are not related to the mass of the peptide, were detected in the $\text{Ac-KG}_5\text{F}_3\text{-CONH}_2$ spectrum: 318.19 m/z ($[\text{M}+3\text{Na}]^{3+}$), 478.87 m/z ($[\text{M}+2\text{ACN}+2\text{H}]^{2+}$), 486.38 m/z ($[\text{M}+3\text{ACN}+2\text{H}]^{2+}$) and 972.5 m/z ($[\text{M}+\text{ACN}+\text{Na}]^+$). Those peaks are derived from the interactions between peptide ions with the solvents or other ions presents on the MS.

The MS results of $\text{Ac-K}_2\text{G}_5\text{F-CONH}_2$ and $\text{Ac-K}_2\text{G}_7\text{F}_4\text{-CONH}_2$ reveal two major peaks at 748.70 and 1304.12 m/z ($[\text{M}+\text{H}]^+$) and at 374.99 and 652.81 m/z ($[\text{M}+2\text{H}]^{2+}$), respectively. These peaks correspond to two ionization states, as each peptide has only two positively charged amino acids.

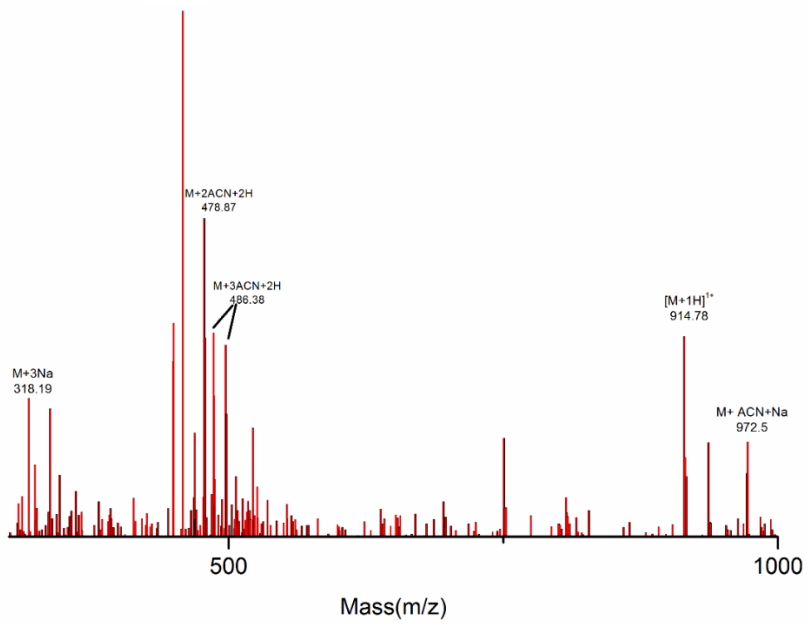
The spectrum of $\text{Ac-K}_3\text{G}_5\text{F}_3\text{-CONH}_2$ illustrates three major peaks of $[\text{M}+\text{H}]^+$ (1172.13 m/z), $[\text{M}+2\text{H}]^{2+}$ (586.36 m/z) and $[\text{M}+3\text{H}]^{3+}$ (391.42 m/z), that are associated to the three ionization states of the peptide. Furthermore, other peaks are present in the spectrum, such as at 605.35 m/z ($[\text{M}+2\text{ACN}+2\text{H}]^{2+}$), which resulted from interactions between peptide ions with MS solvents.

Lastly, comparing the MS results with the possible m/z values shown on table 3.2, it is concluded that the right peptides were synthesised.

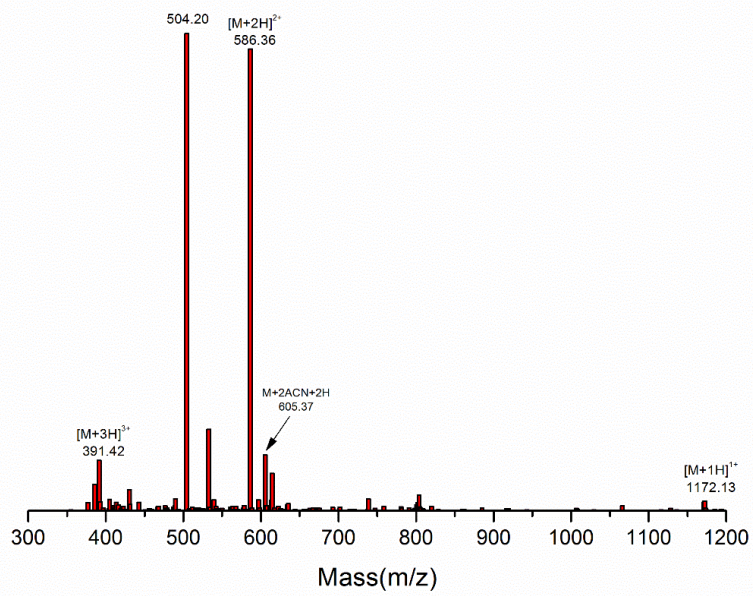




Ac-KG₅F₃-CONH₂



Ac-K₃G₅F₃-CONH₂



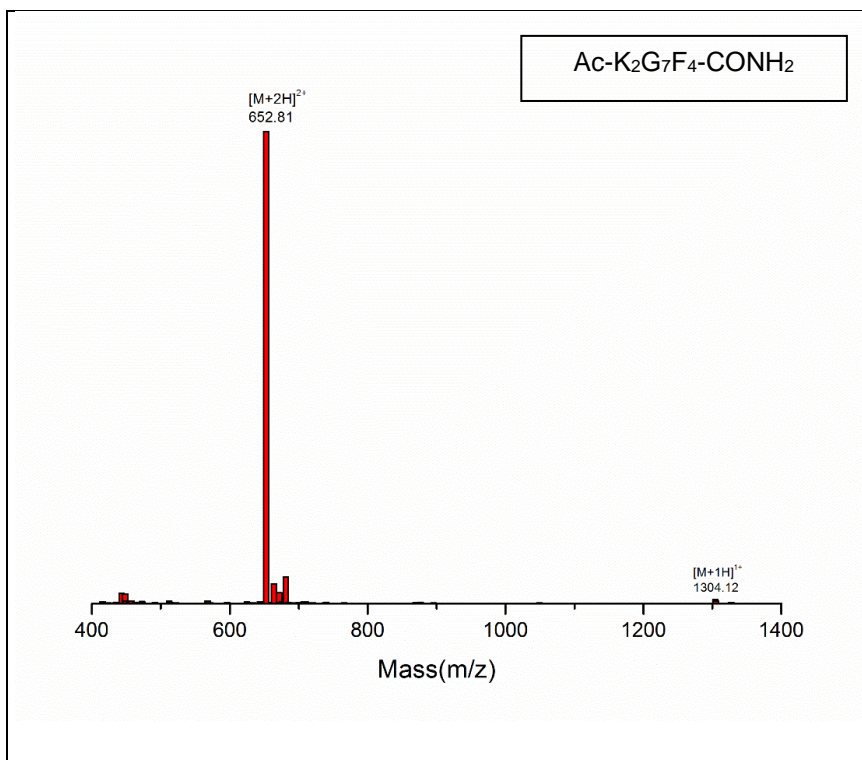


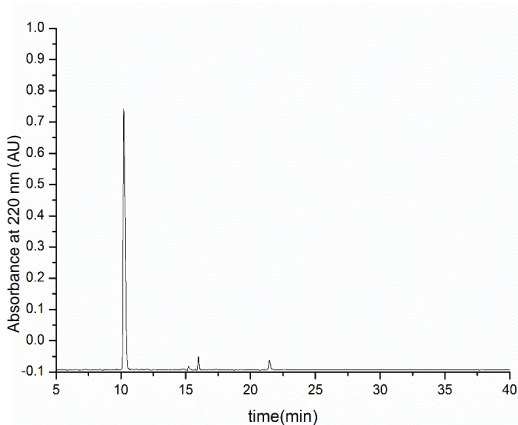
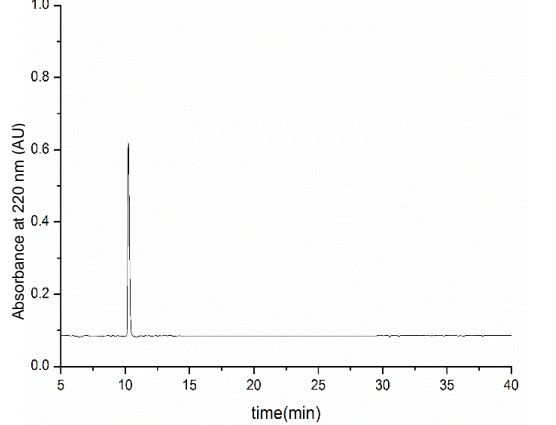
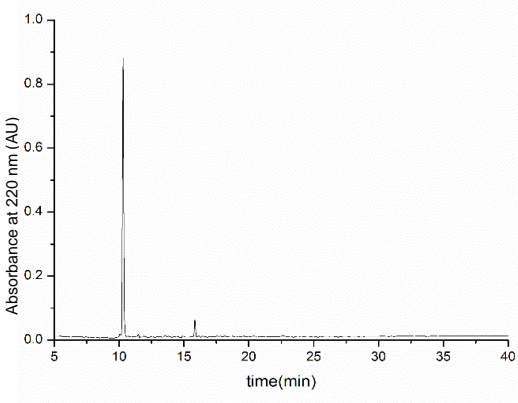
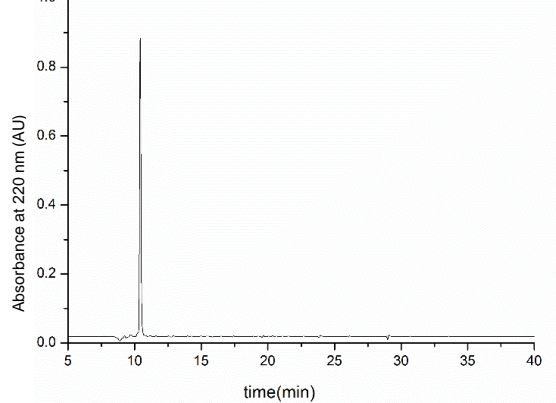
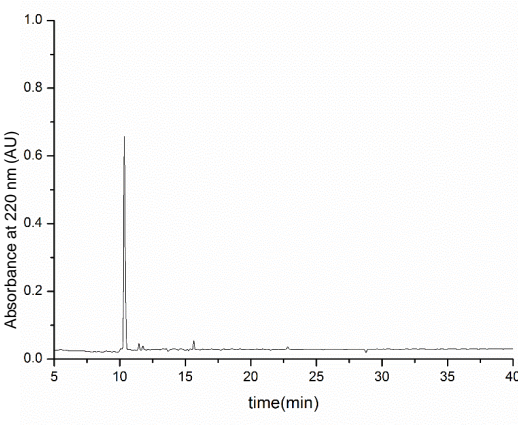
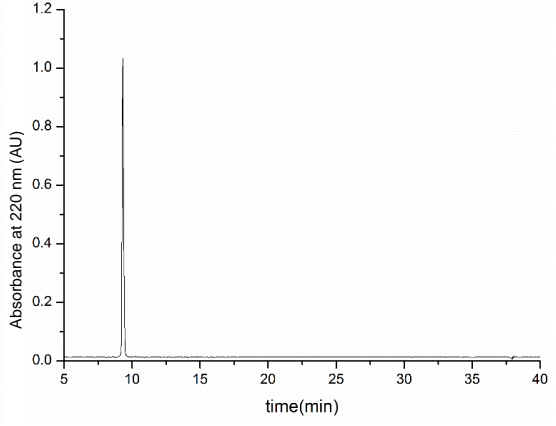
Figure 3.1- Mass-spectrometry analysis of the synthesised peptides.

2.2) HPLC

In order to analyse the purity of the peptides, samples were injected into an analytic HPLC system and eluted with a gradient of water/ACN as mobile phase. The figure 3.2 represent the HPLC analysis before and after purification of the synthesised peptides.

According to the results, the peak of the peptides $\text{NH}_2\text{-KG}_2\text{F-CONH}_2$, $\text{Ac-KG}_5\text{F-CONH}_2$ and $\text{Ac-K}_2\text{G}_5\text{F-CONH}_2$ elutes at 10 minutes and for the peptides $\text{Ac-KG}_5\text{F}_3\text{-CONH}_2$, $\text{Ac-K}_3\text{G}_5\text{F}_3\text{-CONH}_2$ and $\text{Ac-K}_2\text{G}_7\text{F}_4\text{-CONH}_2$ the peak elutes after 15 minutes. These results are in correlation with the increasing in number of aromatic residues in the sequence. Since the column is hydrophobic, increasing the number of hydrophobic residues in the sequence will result in longer elution times.

On the graphs before the purification, besides the peak with higher intensity, smaller peaks are detected due to the presence of some impurities in the peptides. However, the results after purification only reveal a single peak that is related to the peptide. Therefore, comparing the graphs before and after purification, it is concluded that all peptides are almost 99% pure.

Peptides	Crude peptide	Pure peptide
<p>NH₂- KG₂F- CONH₂</p>	 <p>Absorbance at 220 nm (AU)</p> <p>time(min)</p>	 <p>Absorbance at 220 nm (AU)</p> <p>time(min)</p>
<p>Ac-KG₅F- CONH₂</p>	 <p>Absorbance at 220 nm (AU)</p> <p>time(min)</p>	 <p>Absorbance at 220 nm (AU)</p> <p>time(min)</p>
<p>Ac-K₂G₅F- CONH₂</p>	 <p>Absorbance at 220 nm (AU)</p> <p>time(min)</p>	 <p>Absorbance at 220 nm (AU)</p> <p>time(min)</p>

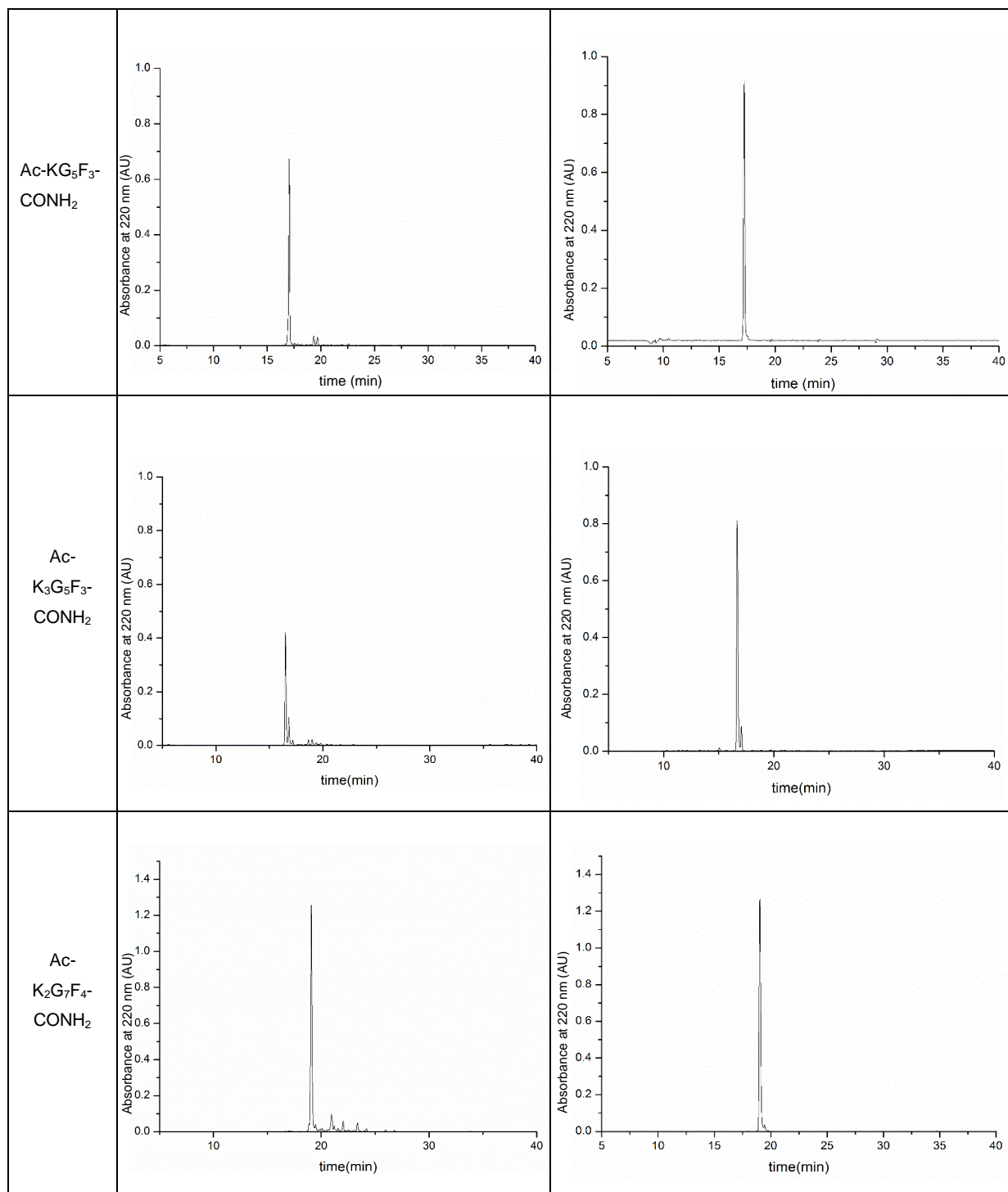


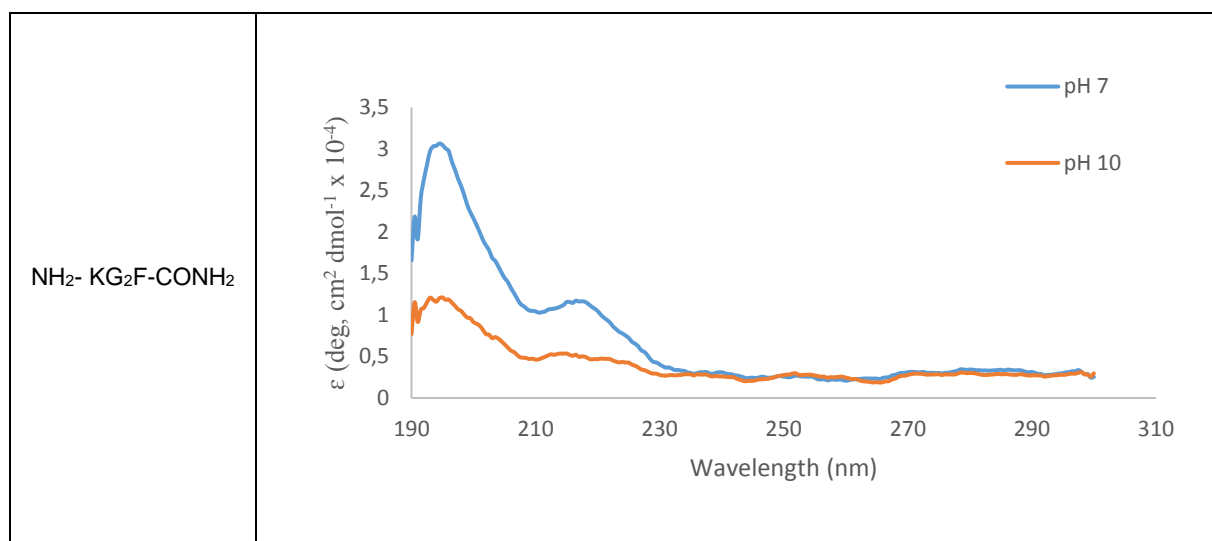
Figure 3.2- HPLC analysis before and after purification for the synthesised peptides.

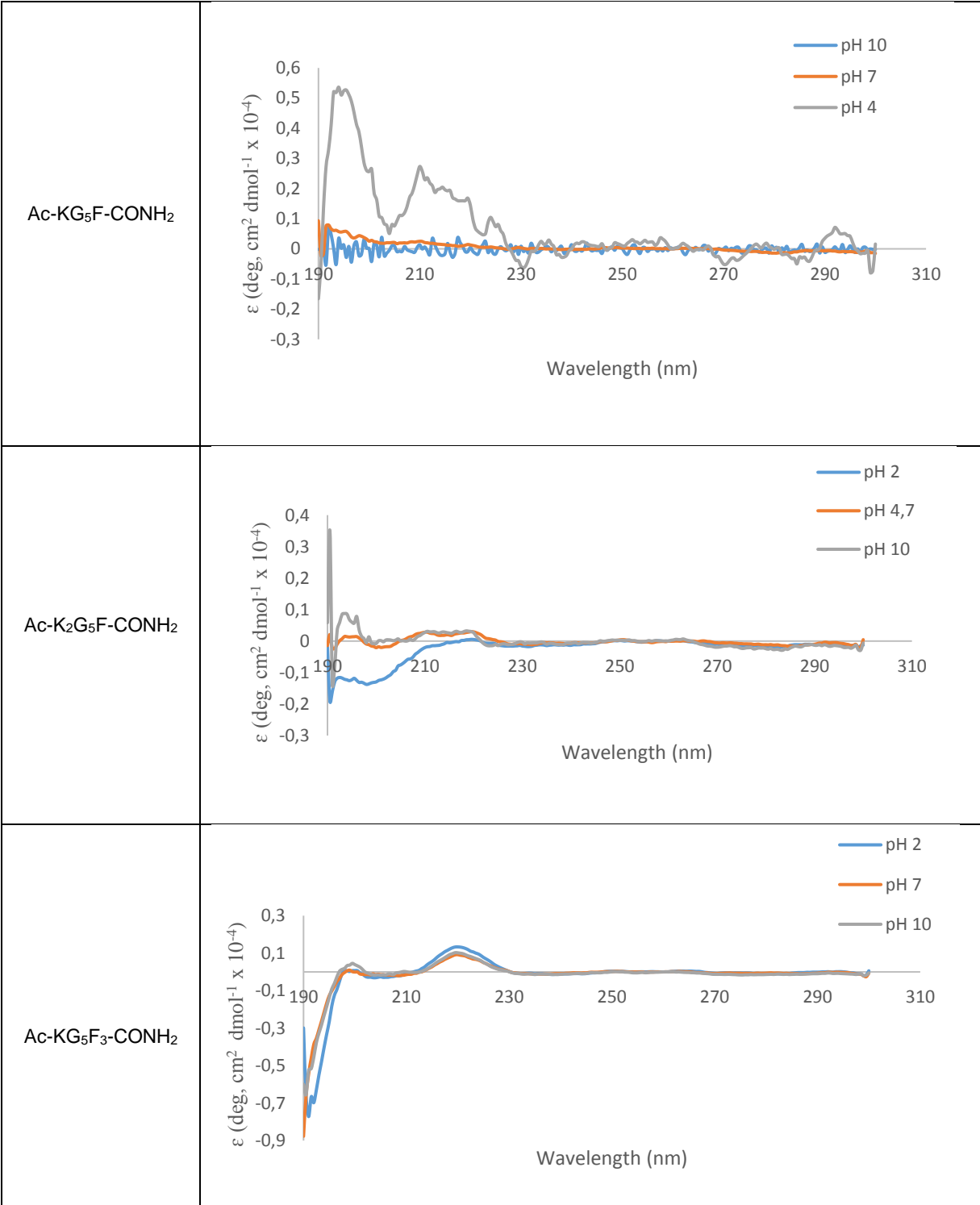
2.3) CD

CD spectroscopy was performed to analyse the secondary structure of the synthesised peptides in different pHs. Diverse types of secondary structures in peptides originate distinct types of far UV CD spectra, which depends on the length and regularity of structural elements in peptides (Kelly & Price, 2000). The CD spectra can be influenced by several factors, such as the rigidity of the peptide, the nature of the environment in terms of hydrogen bonding, polar groups and polarizability and aromatic

rings (Kelly & Price, 2000). A CD standard curve is shown in figure 3.4 which acts as a support and reference for interpretation of the CD results present in figure 3.3.

Comparing to the standard graph, the peptides $\text{NH}_2\text{-KG}_2\text{F-CONH}_2$, $\text{Ac-KG}_5\text{F-CONH}_2$, $\text{Ac-K}_2\text{G}_5\text{F-CONH}_2$ do not show any specific secondary structure such as β -sheet, α -helix or random coil structures. These results can be related with the glycines present on the peptides, once it is the only non-chiral amino acid and a CD signal is only observed when a chromophore is chiral (optically active). For that reason, glycine can interfere on the CD signal. Respite the irregular behaviour, the peptides $\text{Ac-KG}_5\text{F}_3\text{-CONH}_2$ and $\text{Ac-K}_3\text{G}_5\text{F}_3\text{-CONH}_2$ show structures similar to random coil for the three pHs. This abnormal behaviour can be associated to the glycines or to the aromatic rings of the phenylalanines. The CD spectrum can be altered by interactions between aromatic rings and this effect may be especially significant if the distance between them is less than 1 nm (Kelly & Price, 2000). Furthermore, as much of such amino acids are added to the peptide sequence, smaller CD bands are expected due to the cancelling effects of positive and negative contributions (Kelly & Price, 2000). Lastly, the peptide $\text{Ac-K}_2\text{G}_7\text{F}_4\text{-CONH}_2$ reveals structures similar to random coil for pHs 4 and 8 and β -sheet for the pH 10; however, the curve of the peptide starts with lower ellipticity than the β -sheet standard curve, as well as the large peak that has higher ellipticity.





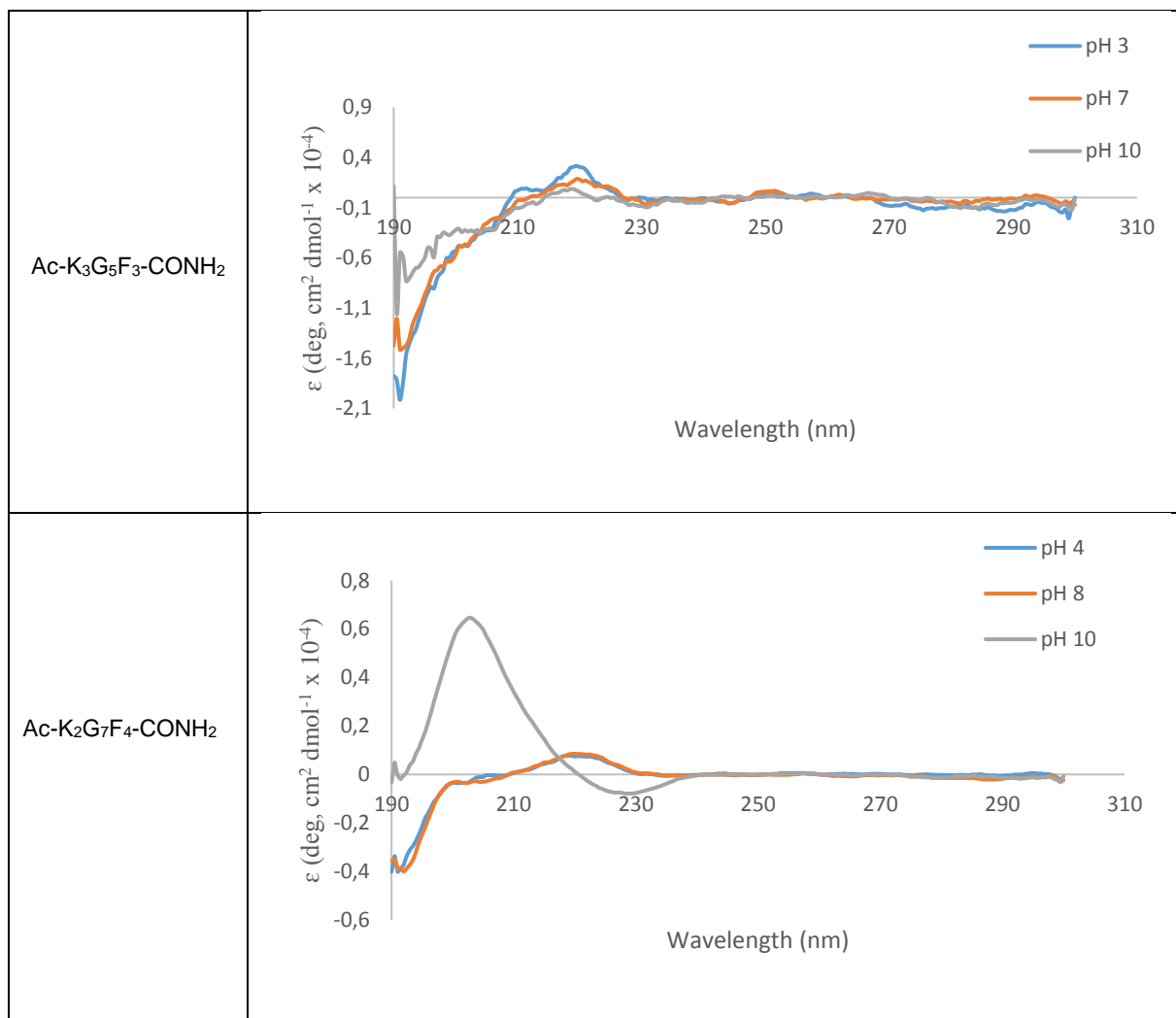


Figure 3.3- CD spectroscopy analysis for the synthesised peptides.

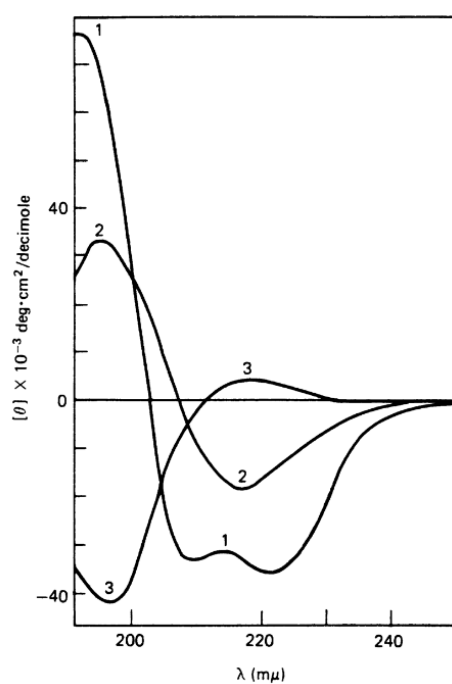


Figure 3.4- CD standard curve: 1) α -helix, 2) β -sheet and 3) random coil (Greenfield & Fasman, 1969).

3) Peptide-HA hydrogels preparation

▪ $\text{NH}_2\text{-KG}_2\text{F-CONH}_2$ (P1), $\text{Ac-KG}_5\text{F-CONH}_2$ (P2) and $\text{Ac-K}_3\text{G}_5\text{F}_3\text{-CONH}_2$ (P5)

The gel formation was investigated during 1 week and no interactions were observed for the gel testing of the peptides $\text{NH}_2\text{-KG}_2\text{F-CONH}_2$, $\text{Ac-KG}_5\text{F-CONH}_2$ and $\text{Ac-K}_3\text{G}_5\text{F}_3\text{-CONH}_2$. This can be related to the insufficient number of positively charged (lysine) and aromatic (phenylalanine) amino acids present on the peptides, once gel formation depends of electrostatic interactions between positively charged amino acids and HA (negatively charged) and π - π stacking between aromatic rings of the peptides. Also, electrostatic interactions have higher energy (250 kJ mol^{-1}) when comparing with π - π stacking ($0\text{-}50 \text{ kJ mol}^{-1}$), thus, possibly, it is necessary to have a higher number of phenylalanines than lysines to obtain hydrogels (Mendes et al., 2013). The lower concentrations (2% w/v) of the peptide and HA solutions that were used can also justified these results. However, even for higher peptide solution concentration (10% w/v) and testing the peptide in powder form, no gel formation were observed for $\text{Ac-KG}_5\text{F-CONH}_2$ and $\text{Ac-K}_3\text{G}_5\text{F}_3\text{-CONH}_2$.

▪ $\text{Ac-K}_2\text{G}_5\text{F-CONH}_2$ (P3)

For the gel testing represented on table 2.5, a peptide solution with pH 3 was used. It was expected that in a presence of an acidic solution the positive charges of lysine become more positive, thus increasing the interactions between the peptide and HA (negatively charged). Although, neither for acidic peptide solution or neutral peptide solution, no interactions between the peptides and HA and consequently no gel formation were observed. Also, when a higher peptide solution (10% w/v) was combined with 700 kDa HA (2%), no gel formation were detected (figure 2.1). This may be related with the absence of π - π interactions once the present peptide has only one phenylalanine in its sequence. For the experiments shown in table 2.6, only one positive result for gel formation were observed (figure 3.5); when 0.005 g of $\text{Ac-K}_2\text{G}_5\text{F-CONH}_2$ in powder form was combined with 50 μl of 700 kDa HA solution (2%), a soft gel was formed. In order to test its stability, ultrapure water was added to the gel. However the gel was not stable and, thus, it was impossible to prepare it for the SEM.



Figure 3.5- $\text{Ac-K}_2\text{G}_5\text{F-CONH}_2$ gel formation results: soft gel.

▪ **Ac-KG₅F₃-CONH₂ (P4)**

The figure 3.6 shows the results of the gel testing represented on figure 2.3. The combination of a peptide solution (10% w/v) with HA solutions of different molecular weights resulted in a stable membrane (700 kDa HA) and in a precipitated solution (60 kDa HA). Furthermore, the 20% (w/v) peptide solution resulted in a soft gel after one day in a water bath at 60 °C. Thus, HA with higher molecular weights seems to induce the gel formation. However, the gel was not strong enough for characterization by SEM. On the contrary, the membrane was stable.


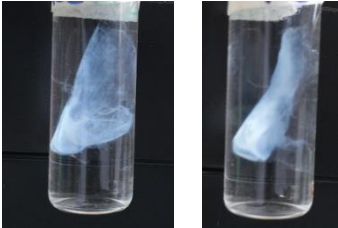
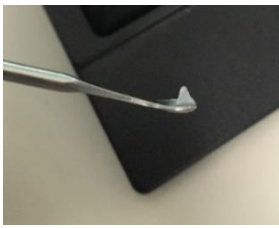








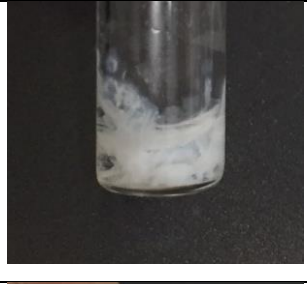





	50 µl P4 + 50 µl HA 60 kDa (2%)	20 µl P4 + 20 µl HA 700 kDa (2%)	P4 (20% w/v)
Observations	Precipitation	Membrane	Soft gel
Results			

Figure 3.6- Gel formation investigation results for Ac-KG₅F₃-CONH₂.

The figure 3.7 represents the results of the experiments showed on table 2.8. According to the results, it is concluded that the combination of Ac-KG₅F₃-CONH₂ in the powder form with 2% and 1% (w/v) HA solutions of different molecular weights induce the gel formation at higher temperature (60 °C) after 4 hours; with exception for 0.005 g Ac-KG₅F₃-CONH₂ combined with 60 kDa HA (2%) that formed a precipitated solution. However, no gel formation was observed at room temperature for these combinations. The stability of the formed gels in water was tested. After 24 hours of testing, the gels proved to be stable and, thus, able to be characterized by SEM.

	Day 1 (room temperature)	Day 2 (60°C)	Observations
700 kDa HA (2%)			Gel formation was observed

<p>200 kDa HA (2%)</p>			<p>Gel formation was observed</p>
<p>60 kDa HA (2%)</p>			<p>Precipitation was observed</p>
<p>20 kDa HA (2%)</p>			<p>Gel formation was observed</p>
<p>700 kDa HA (1%)</p>			<p>Gel formation was observed</p>
<p>200 kDa HA (1%)</p>			<p>Gel formation was observed</p>
<p>60 kDa HA (1%)</p>			<p>Gel formation was observed</p>





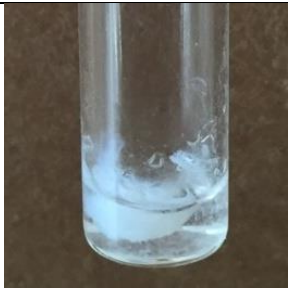



<p>20 kDa HA (1%)</p>			<p>Gel formation was observed</p>
---------------------------	---	--	-----------------------------------

Figure 3.7- Gel formation results for Ac-KG₅F₃-CONH₂ with 2% and 1% HA solution.

▪ **Ac-K₂G₇F₄-CONH₂ (P6)**

The figure 3.8 reveals the results of the gel testing showed on table 2.10. Through the analysis of the results, it is concluded that Ac-K₂G₇F₄-CONH₂ in powder form combined with 700, 200 and 60 kDa 2% (w/v) HA solutions form stable gels, after 4 hours at 60 °C. For 20 kDa 2% (w/v) HA solution, gel formation was not observed, as well as for all experiments at room temperature. Moreover, 20% (w/v) peptide solution showed to form a stable gel too.

	Day 1 (room temperature)	Day 2 (60°C)	Observations
<p>700 kDa HA (2%)</p>			<p>Gel formation was observed</p>
<p>200 kDa HA (2%)</p>			<p>Gel formation was observed</p>
<p>60 kDa HA (2%)</p>			<p>Gel formation was observed</p>





<p>20 kDa HA (2%)</p>			<p>Precipitation was observed</p>
<p>P6 (20% w/v)</p>			<p>Gel formation was observed</p>

Figure 3.8- Gel formation results for Ac-K₂G₇F₄-CONH₂.

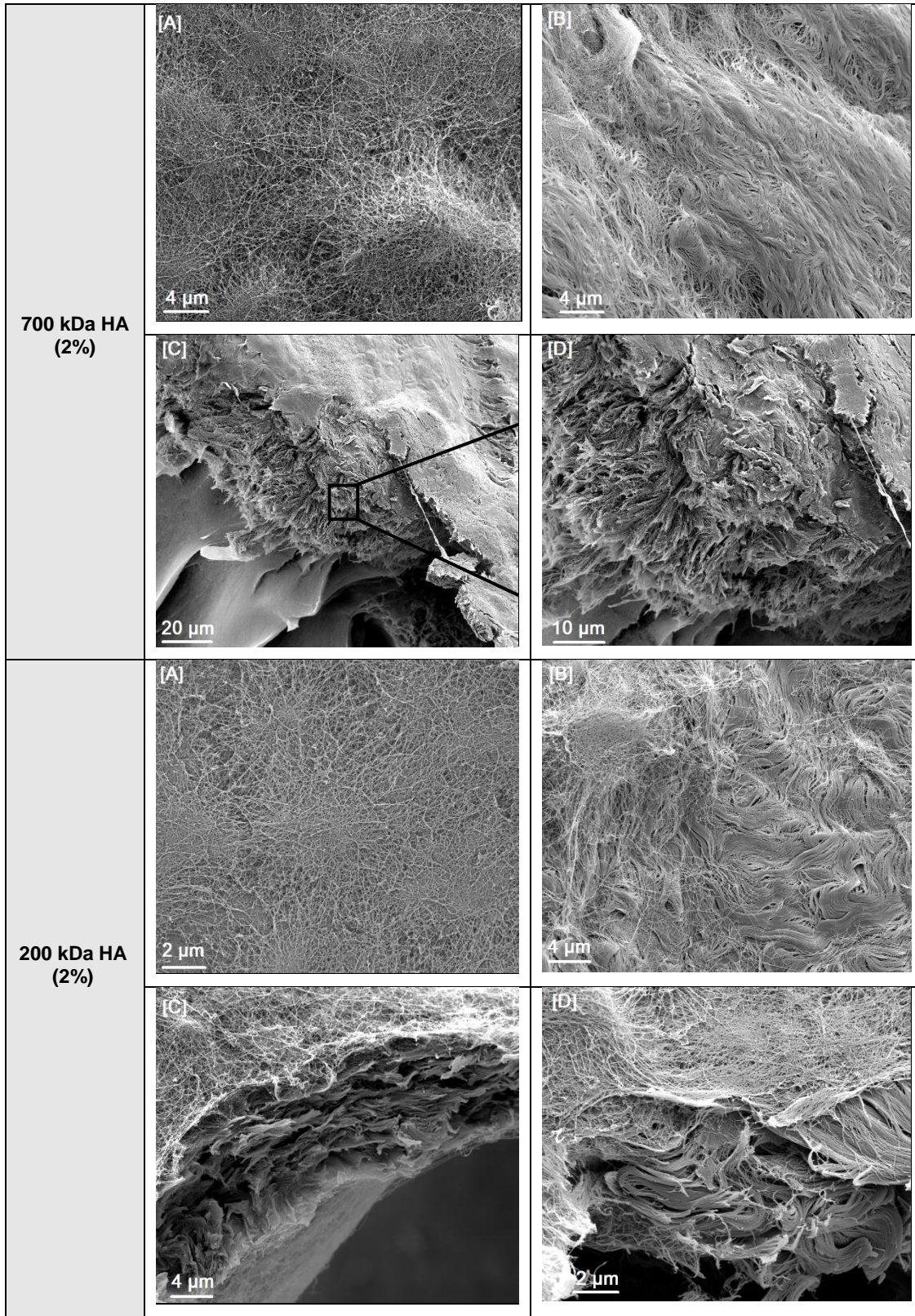
4) Peptide-HA hydrogels characterization

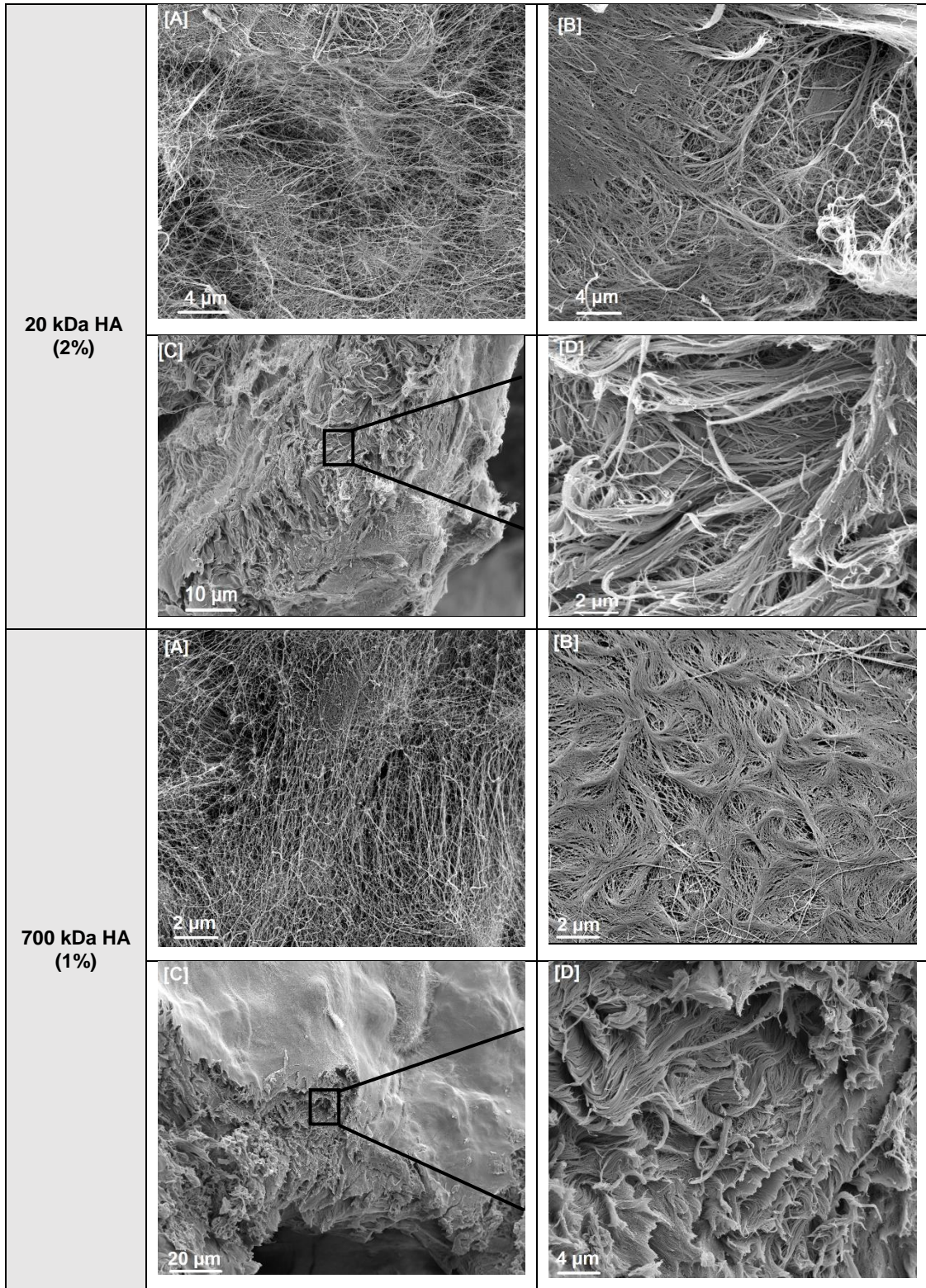
Only the microstructure of the obtained hydrogels was characterized by Scanning Electron Microscopy (SEM); the structure of the membrane was not characterized once the aim of this project was to obtain hydrogels. The results and discussion are described in this point.

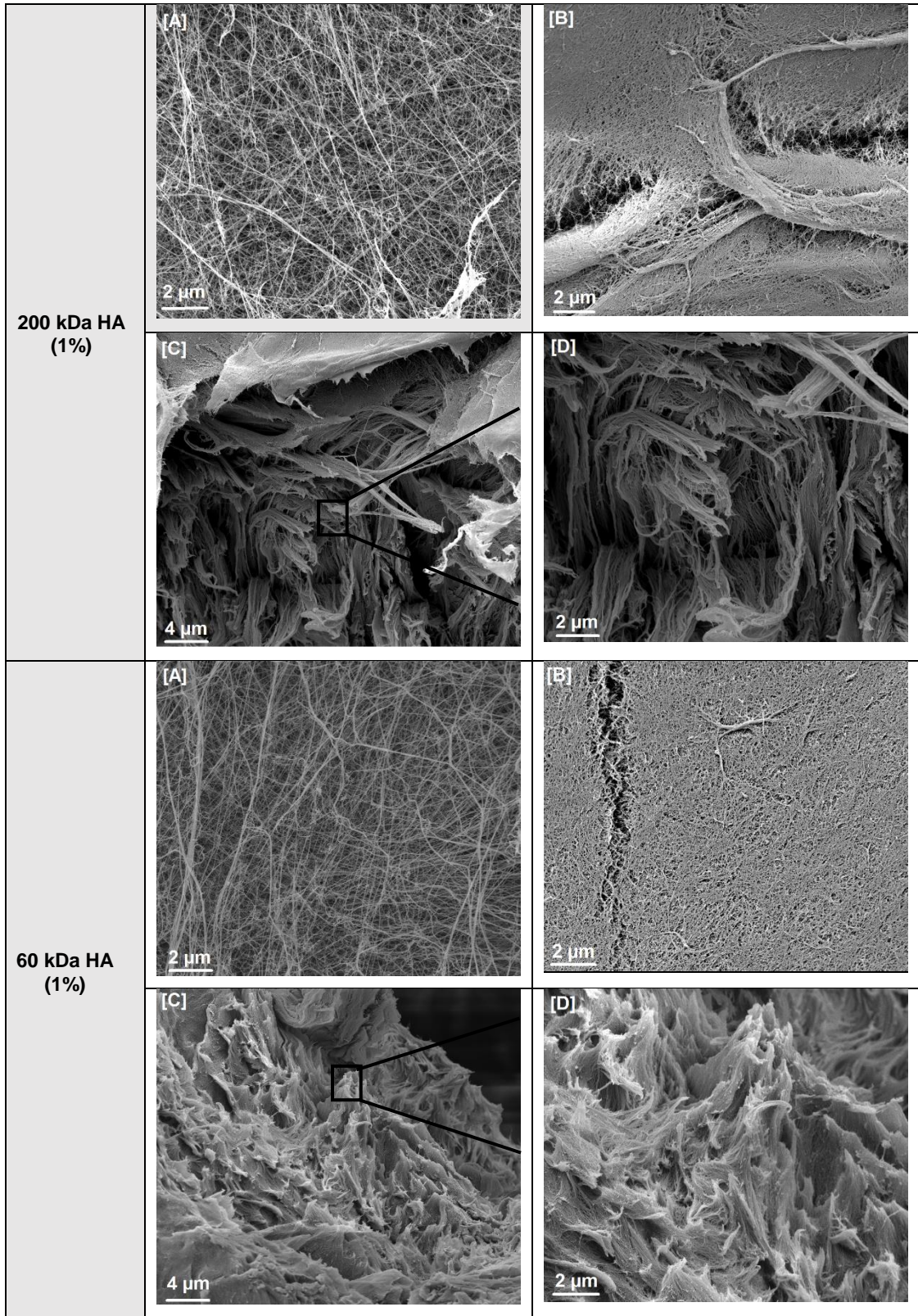
4.1) SEM

▪ Ac-KG₅F₃-CONH₂ (P4)

The microstructures of the Ac-KG₅F₃-CONH₂ with 2% and 1% (w/v) HA gels were characterized by SEM and the images are shown on figure 3.9. According with SEM analysis, the hydrogels reveal a network of nanofibrous structures randomly distributed for 2% and 1% (w/v) HA solutions. In hydrogels with 2% (w/v) HA solution, the molecular weight of the HA had an effect on the packing of the fibers. Lower molecular weight HA (20 kDa) reveals less denser fibers when comparing with higher molecular weight HA (700 and 200 kDa). Also, on one side of the hydrogels with 700 and 200 kDa 2% (w/v) HA, the nanofibrous structures are similar to the ones observed by Gazit et. al (spaghetti-like showed on figure 1.5 d). This similarity might be derived by phenylalanines present on the sequences of the two peptides. For the hydrogels with 1 % (w/v) HA solutions, the difference on the density of the fibers between higher molecular weight (700 kDa) HA solutions and lower (200, 60 and 20 kDa) are visible too. Furthermore, with exception of 700 kDa HA, the hydrogels with 1% (w/v) HA show a network of nanofibrous structures less denser than 2% (w/v) HA hydrogels.







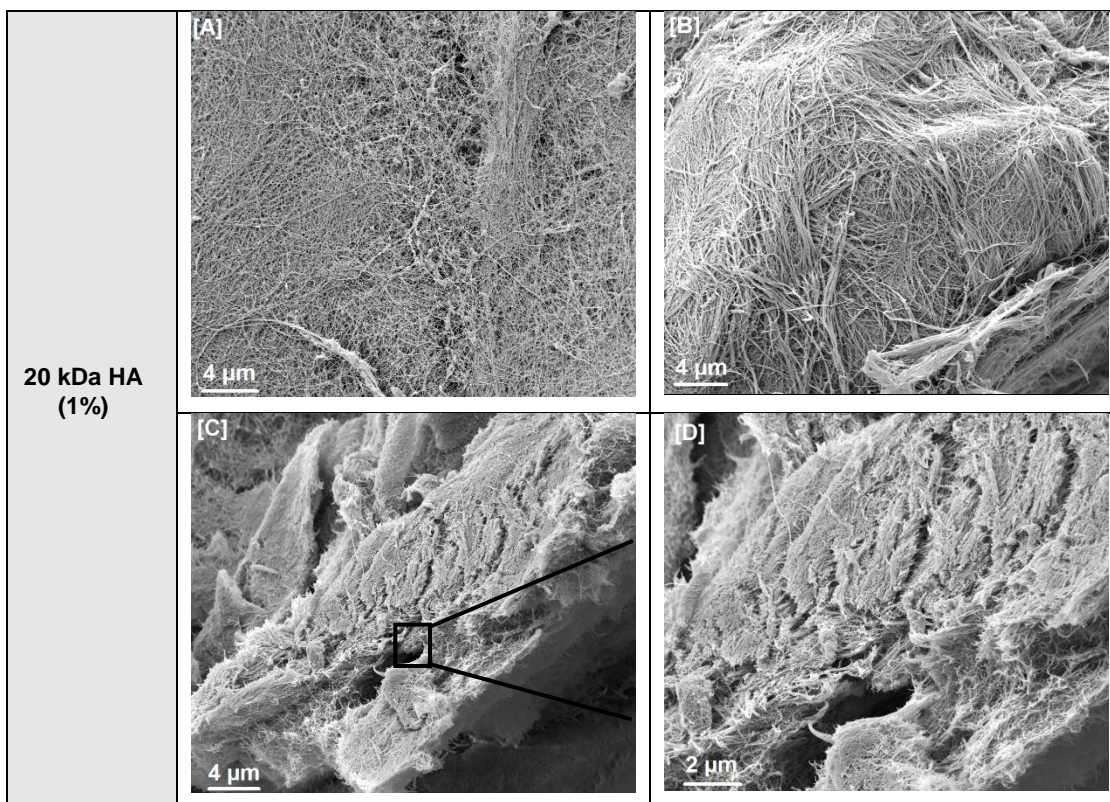
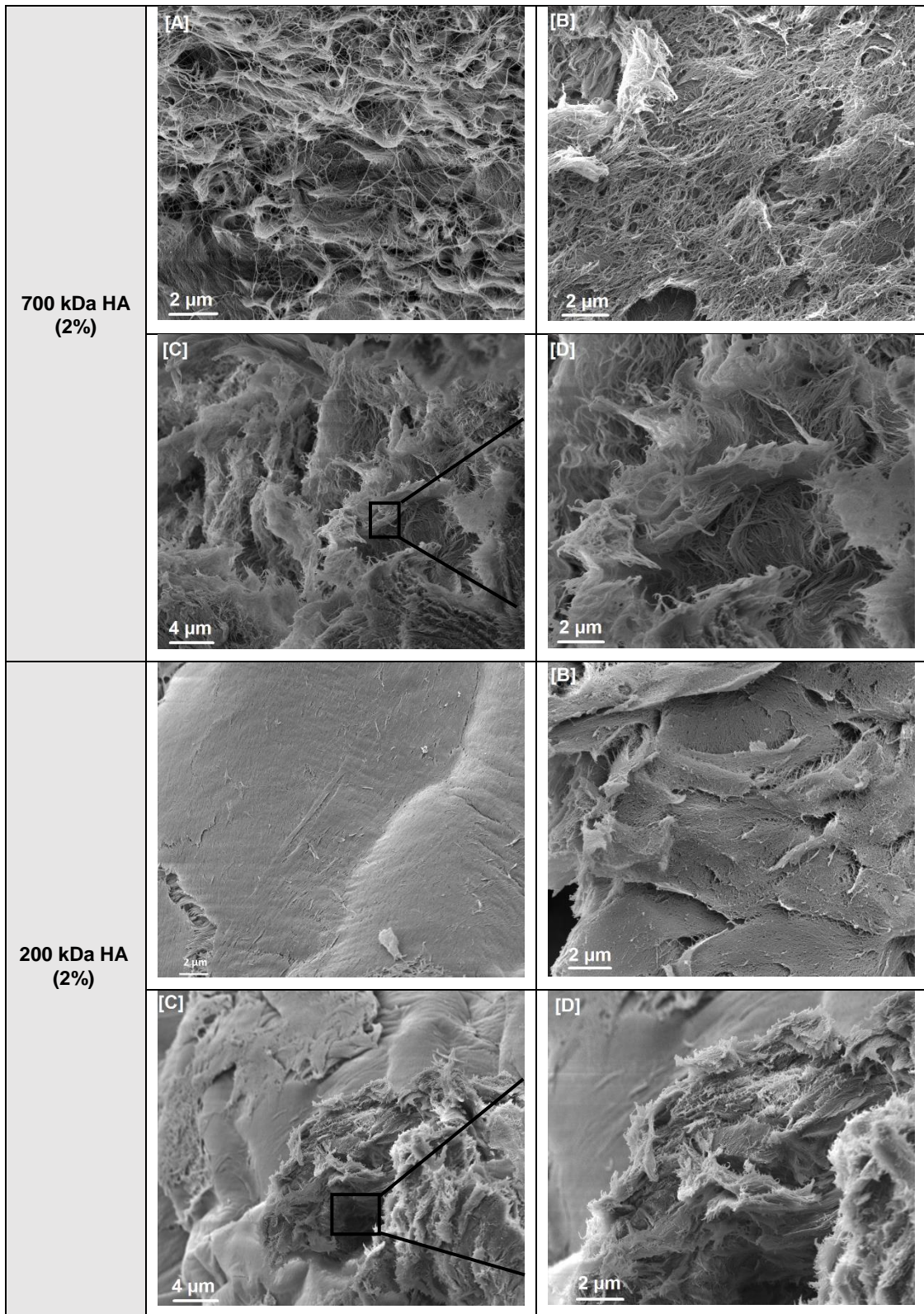


Figure 3.9- SEM images of Ac-KG₅F₃-CONH₂ hydrogels microstructure for 2% HA (700, 200 and 20 kDa) and 1% HA (700, 200, 60 and 20); [A] one side, [B] other side, [C] and [D] cross-section.

- **Ac-K₂G₇F₄-CONH₂ (P6)**

Figure 3.10 shows the SEM analysis for Ac-K₂G₇F₄-CONH₂ and HA hydrogels microstructure presented on figure 3.8. Comparing with Ac-KG₅F₃-CONH₂, the hydrogels show denser and more organized (200 kDa and 20% P6) fibrous structure. These might be related with the the peptide sequence. Once this peptide has a higher number of phenylalanines and lysines, it was expected that the hydrogels were more consistent and stronger with respect to the higher electrostatic and π-π stacking interactions. In contrast to the Ac-KG₅F₃-CONH₂ gels, these hydrogels (figure 3.10) showed homogenous structures, as the two sides ([A] and [B]) of the gels are very similar, revealing the same type of structure. This may be related to the stronger electrostatic interactions compared to the Ac-KG₅F₃-CONH₂/HA gels, which the aromatic interactions seem to be dominant. Finally, hydrogel with 200 kDa HA and the 20% (w/v) peptide solution have more organized structures than the other hydrogels (700 and 60 kDa), that shows random structures.



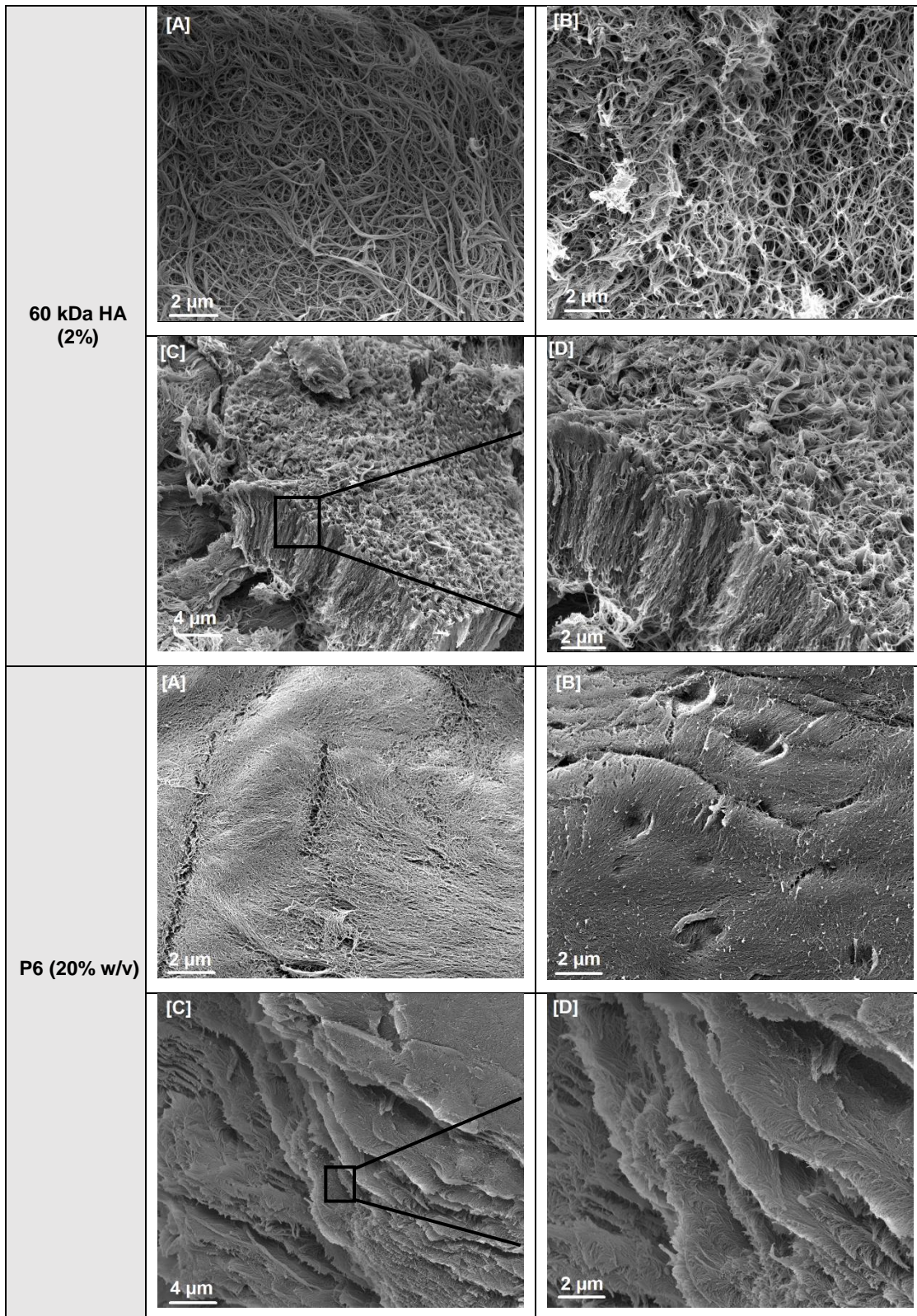


Figure 3.10- SEM images for Ac-K₂G₇F₄-CONH₂ hydrogels microstructure for 20% w/v and 2% HA: 700, 200 and 60 kDa; [A] one side, [B] other side, [C] and [D] cross-section.

CHAPTER 4: Conclusion and future work

1) Conclusion

In the present study, the development of a novel hyaluronan base hydrogel obtained by supramolecular crosslinking with peptides was investigated. For this purpose, the peptides NH₂-KG₂F-CONH₂, Ac-KG₅F-CONH₂, Ac-K₂G₅F-CONH₂, Ac-KG₅F₃-CONH₂, Ac-K₃G₅F₃-CONH₂ and Ac-K₂G₇F₄-CONH₂ were successfully synthesized by the Fmoc protocol and were purified by HPLC. Their mass was confirmed by ESI-MS. The secondary structure of the peptides was analysed with circular dichroism spectroscopy. The peptides NH₂-KG₂F-CONH₂, Ac-KG₅F-CONH₂, Ac-K₂G₅F-CONH₂ did not show any specific secondary structure such as β -sheet, α -helix or random coil structures and the peptides Ac-KG₅F₃-CONH₂, Ac-K₃G₅F₃-CONH₂ and Ac-K₂G₇F₄-CONH₂ showed structures similar to random coil and β -sheet. This can be related to the interference of glycines and phenylalanines on the CD spectra, once characteristics of the spectra can depend on the length and regularity of structural elements in peptides.

In order to investigate hydrogel formation, the peptides were combined with HA solutions in different combinations. Diverse concentrations of HA solutions with different molecular weights were tested with the peptides in powder form or in solution, expecting interactions between the peptides and hyaluronan to induce gel formation. After all the experiments, only for the peptides Ac-KG₅F₃-CONH₂ and Ac-K₂G₇F₄-CONH₂ positive results for gel formation were observed. The peptide Ac-KG₅F₃-CONH₂ in powder form combined with 2% and 1% (w/v) HA solutions of 700, 200, 60 and 20 kDa can self-assemble and form stable gels with fibrous structures randomly distributed confirmed by SEM images. Moreover, for the 2% (w/v) HA, the molecular weight showed to have effect on packing of the fibers. Hydrogels with lower molecular weight HA reveals less denser fibers when comparing with higher molecular weight. Also, the peptide Ac-K₂G₇F₄-CONH₂ in powder form combined with ultrapure water (20% w/v) and with 2% (w/v) HA solutions of 60, 200 and 700 kDa self-assembled into stable gels. The characterization of the hydrogels by SEM showed denser, more organized and homogenous structures than the Ac-KG₅F₃-CONH₂/HA hydrogels structures.

In conclusion, the sequence of the peptide, the concentration of the HA and peptide solutions, the different molecular weights HA and the peptide in powder form showed to influence the hydrogel formation; as well as to have an effect on the density and packing of the fibers of the obtained hydrogels structures.

2) Future work

The self-assembly between peptides, with design based on the ABC block, which A corresponds to a charged residue (lysine), B a spacer (such as glycine) and C an aromatic residue (phenylalanine), and HA showed to form stable hydrogels. However, more investigations are required to analyse in detail some aspects. Future studies will be focus on topics of the following list.

- Analysis of the mechanical proprieties of the hydrogels through rheology studies;
- Analysis of hydrogels properties for biomedical applications, such as cell culture to determine if the gels support cell survival and proliferation;

- Investigating the hydrogel formation for peptides with different spacer, such as alanine or serine, and then characterized its microstructures by SEM and mechanical properties.

Peptide self-assembly has been considered a great method to develop new scaffolds, bringing new opportunities for tissue engineering and regenerative medicine.

APPENDIX

1) Yield Calculations

▪ KG_5F

$$\frac{0.25}{1000} \text{ mol} \times 619.68 \frac{\text{gr}}{\text{mol}} = 0.1549 \text{ gr}$$

$$\text{yiel (\%)} = \frac{0.1242 \text{ gr}}{0.1549 \text{ gr}} \times 100\% = 80.2\%$$

▪ $\text{K}_2\text{G}_5\text{F}$

$$\frac{0.5}{1000} \text{ mol} \times 747.86 \frac{\text{gr}}{\text{mol}} = 0.3739 \text{ gr}$$

$$\text{yiel (\%)} = \frac{0.3601 \text{ gr}}{0.3739 \text{ gr}} \times 100\% = 96.3\%$$

▪ KG_5F_3

$$\frac{0.25}{1000} \text{ mol} \times 914.03 \frac{\text{gr}}{\text{mol}} = 0.2285 \text{ gr}$$

$$\text{yiel (\%)} = \frac{0.1934 \text{ gr}}{0.2285 \text{ gr}} \times 100\% = 84.6\%$$

▪ $\text{K}_3\text{G}_5\text{F}_3$

$$\frac{0.25}{1000} \text{ mol} \times 1170.38 \frac{\text{gr}}{\text{mol}} = 0.2926 \text{ gr}$$

$$\text{yiel (\%)} = \frac{0.1962 \text{ gr}}{0.2926 \text{ gr}} \times 100\% = 67.1\%$$

▪ $\text{K}_2\text{G}_7\text{F}_4$

$$\frac{0.5}{1000} \text{ mol} \times 1303.49 \frac{\text{gr}}{\text{mol}} = 0.6517 \text{ gr}$$

$$\text{yiel (\%)} = \frac{0.6241 \text{ gr}}{0.6517 \text{ gr}} \times 100\% = 95.8\%$$

References

- Aguilar, M.-I. (2004). Reversed-phase high-performance liquid chromatography. *HPLC of peptides and proteins: Methods and protocols*, 9-22.
- Aguilar, M.-I., & Hearn, M. T. (1996). High-resolution reversed-phase high-performance liquid chromatography of peptides and proteins. *Methods in enzymology*, 270, 3-26.
- Barany, G., Kneib-Cordonier, N., & Mullen, D. G. (1987). Solid-phase peptide synthesis: a silver anniversary report. *International journal of peptide and protein research*, 30(6), 705-739.
- Bishop, K. J., Campbell, C. J., Mahmud, G., & Grzybowski, B. A. (2008). Biomimetic Design of Dynamic Self-Assembling Systems. *Studies in Multidisciplinarity*, 5, 21-48.
- Burdick, J. A., & Prestwich, G. D. (2011). Hyaluronic acid hydrogels for biomedical applications. *Advanced Materials*, 23(12).
- Capito, R. M., Azevedo, H. S., Velichko, Y. S., Mata, A., & Stupp, S. I. (2008). Self-assembly of large and small molecules into hierarchically ordered sacs and membranes. *Science*, 319(5871), 1812-1816.
- Caplan, M. R., Moore, P. N., Zhang, S., Kamm, R. D., & Lauffenburger, D. A. (2000). Self-assembly of a β -sheet protein governed by relief of electrostatic repulsion relative to van der Waals attraction. *Biomacromolecules*, 1(4), 627-631.
- Chatterjea, M., & Shinde, R. (2011). *Textbook of medical biochemistry: Wife Goes On*.
- Cherny, I., & Gazit, E. (2008). Amyloids: not only pathological agents but also ordered nanomaterials. *Angewandte Chemie International Edition*, 47(22), 4062-4069.
- Chow, L. W., Bitton, R., Webber, M. J., Carvajal, D., Shull, K. R., Sharma, A. K., & Stupp, S. I. (2011). A bioactive self-assembled membrane to promote angiogenesis. *Biomaterials*, 32(6), 1574-1582.
- Claessens, C. G., & Stoddart, J. F. (1997). REVIEW COMMENTARY—INTERACTIONS IN SELF-ASSEMBLY. *Journal of physical organic chemistry*, 10, 254-272.
- Coin, I., Beyermann, M., & Bienert, M. (2007). Solid-phase peptide synthesis: from standard procedures to the synthesis of difficult sequences. *Nature protocols*, 2(12), 3247-3256.
- Dass, C. (2007). *Fundamentals of contemporary mass spectrometry* (Vol. 16): John Wiley & Sons.
- Dawson, P. H. (2013). *Quadrupole mass spectrometry and its applications*: Elsevier.
- Egerton, R. F. (2006). *Physical principles of electron microscopy: an introduction to TEM, SEM, and AEM*: Springer Science & Business Media.
- Engelhardt, H. (2012). *High performance liquid chromatography*: Springer Science & Business Media.
- Ferreira, D. S., Marques, A. P., Reis, R. L., & Azevedo, H. S. (2013). Hyaluronan and self-assembling peptides as building blocks to reconstruct the extracellular environment in skin tissue. *Biomaterials Science*, 1(9), 952-964.
- Ferreira, D. S., Reis, R. L., & Azevedo, H. S. (2013). Peptide-based microcapsules obtained by self-assembly and microfluidics as controlled environments for cell culture. *Soft Matter*, 9(38), 9237. doi: 10.1039/c3sm51189h
- Fournier, A. E., & Strittmatter, S. M. (2001). Repulsive factors and axon regeneration in the CNS. *Current opinion in neurobiology*, 11(1), 89-94.

- Gazit, E. (2002). A possible role for π -stacking in the self-assembly of amyloid fibrils. *The FASEB Journal*, 16(1), 77-83.
- Gazit, E. (2007). Self-assembled peptide nanostructures: the design of molecular building blocks and their technological utilization. *Chemical Society Reviews*, 36(8), 1263-1269.
- Gillard, R. E., Raymo, F. M., & Stoddart, J. F. (1997). Controlling self-assembly. *Chemistry—A European Journal*, 3(12), 1933-1940.
- Glabe, C. G. (2006). Common mechanisms of amyloid oligomer pathogenesis in degenerative disease. *Neurobiology of aging*, 27(4), 570-575.
- Greenfield, N. J., & Fasman, G. D. (1969). Computed circular dichroism spectra for the evaluation of protein conformation. *Biochemistry*, 8(10), 4108-4116.
- Grzybowski, B. A., Wilmer, C. E., Kim, J., Browne, K. P., & Bishop, K. J. (2009). Self-assembly: from crystals to cells. *Soft Matter*, 5(6), 1110-1128.
- Ha, C.-E., & Bhagavan, N. (2011). *Essentials of Medical Biochemistry: With Clinical Cases*: Academic Press.
- Hay, E. D. (2013). *Cell biology of extracellular matrix*: Springer Science & Business Media.
- Holmes, T. C. (2002). Novel peptide-based biomaterial scaffolds for tissue engineering. *TRENDS in Biotechnology*, 20(1), 16-21.
- Hynes, R. O., & Lander, A. D. (1992). Contact and adhesive specificities in the associations, migrations, and targeting of cells and axons. *Cell*, 68(2), 303-322.
- Jameson, J. M., Cauvi, G., Sharp, L. L., Witherden, D. A., & Havran, W. L. (2005). $\gamma\delta$ T cell-induced hyaluronan production by epithelial cells regulates inflammation. *The Journal of experimental medicine*, 201(8), 1269-1279.
- Jayawarna, V., Ali, M., Jowitt, T. A., Miller, A. F., Saiani, A., Gough, J. E., & Ulijn, R. V. (2006). Nanostructured Hydrogels for Three-Dimensional Cell Culture Through Self-Assembly of Fluorenylmethoxycarbonyl-Dipeptides. *Advanced Materials*, 18(5), 611-614.
- Jiang, D., Liang, J., & Noble, P. W. (2007). Hyaluronan in tissue injury and repair. *Annu. Rev. Cell Dev. Biol.*, 23, 435-461.
- Jiang, D., Liang, J., & Noble, P. W. (2011). Hyaluronan as an immune regulator in human diseases. *Physiological reviews*, 91(1), 221-264.
- Kelly, S. M., Jess, T. J., & Price, N. C. (2005). How to study proteins by circular dichroism. *Biochimica et Biophysica Acta (BBA)-Proteins and Proteomics*, 1751(2), 119-139.
- Kelly, S. M., & Price, N. C. (2000). The use of circular dichroism in the investigation of protein structure and function. *Current protein and peptide science*, 1(4), 349-384.
- Mahler, A., Reches, M., Rechter, M., Cohen, S., & Gazit, E. (2006). Rigid, Self-Assembled Hydrogel Composed of a Modified Aromatic Dipeptide. *Advanced Materials*, 18(11), 1365-1370.
- Mandal, D., Shirazi, A. N., & Parang, K. (2014). Self-assembly of peptides to nanostructures. *Organic & biomolecular chemistry*, 12(22), 3544-3561.
- Mant, C. T., & Hodges, R. S. (1996). Analysis of peptides by high-performance liquid chromatography. *Methods in enzymology*, 271, 3-50.
- McGaughey, G. B., Gagné, M., & Rappé, A. K. (1998). π -Stacking interactions alive and well in proteins. *Journal of Biological Chemistry*, 273(25), 15458-15463.

- Mendes, A. C., Baran, E. T., Reis, R. L., & Azevedo, H. S. (2013). Self-assembly in nature: using the principles of nature to create complex nanobiomaterials. *Wiley Interdisciplinary Reviews: Nanomedicine and Nanobiotechnology*, 5(6), 582-612.
- Nelson, D. L., & Cox, M. M. (2008). *Lehninger principles of biochemistry* (Fifth edition ed.). W.H. Freeman and Company Sara Tenney.
- Niece, K. L., Hartgerink, J. D., Donners, J. J., & Stupp, S. I. (2003). Self-assembly combining two bioactive peptide-amphiphile molecules into nanofibers by electrostatic attraction. *Journal of the American Chemical Society*, 125(24), 7146-7147.
- Orbach, R., Mironi-Harpaz, I., Adler-Abramovich, L., Mossou, E., Mitchell, E. P., Forsyth, V. T., . . . Seliktar, D. (2012). The rheological and structural properties of Fmoc-peptide-based hydrogels: the effect of aromatic molecular architecture on self-assembly and physical characteristics. *Langmuir*, 28(4), 2015-2022.
- Rechtes, M., Porat, Y., & Gazit, E. (2002). Amyloid fibril formation by pentapeptide and tetrapeptide fragments of human calcitonin. *Journal of Biological Chemistry*, 277(38), 35475-35480.
- Sacchettini, J. C., & Kelly, J. W. (2002). Therapeutic strategies for human amyloid diseases. *Nature Reviews Drug Discovery*, 1(4), 267-275.
- Savin, T., & Doyle, P. S. (2007). Electrostatically tuned rate of peptide self-assembly resolved by multiple particle tracking. *Soft Matter*, 3(9), 1194-1202.
- Shetty, A. S., Zhang, J., & Moore, J. S. (1996). Aromatic π -stacking in solution as revealed through the aggregation of phenylacetylene macrocycles. *Journal of the American Chemical Society*, 118(5), 1019-1027.
- Smith, A. M., Williams, R. J., Tang, C., Coppo, P., Collins, R. F., Turner, M. L., . . . Ulijn, R. V. (2008). Fmoc-Diphenylalanine Self Assembles to a Hydrogel via a Novel Architecture Based on π - π Interlocked β -Sheets. *Advanced Materials*, 20(1), 37-41.
- Smith, L. J., Fiebig, K. M., Schwalbe, H., & Dobson, C. M. (1996). The concept of a random coil: Residual structure in peptides and denatured proteins. *Folding and Design*, 1(5), R95-R106.
- Smith, R. D., Loo, J. A., Loo, R. R. O., Busman, M., & Udseth, H. R. (1991). Principles and practice of electrospray ionization? mass spectrometry for large polypeptides and proteins. *Mass Spectrometry Reviews*, 10(5), 359-452.
- Sun, S., & Bernstein, E. (1996). Aromatic van der Waals clusters: structure and nonrigidity. *The Journal of Physical Chemistry*, 100(32), 13348-13366.
- Teriete, P., Banerji, S., Noble, M., Blundell, C. D., Wright, A. J., Pickford, A. R., . . . Kahmann, J. D. (2004). Structure of the regulatory hyaluronan binding domain in the inflammatory leukocyte homing receptor CD44. *Molecular cell*, 13(4), 483-496.
- Toole, B. P. (2004). Hyaluronan: from extracellular glue to pericellular cue. *Nature Reviews Cancer*, 4(7), 528-539.
- Whitehouse, C. M., Dreyer, R., Yamashita, M., & Fenn, J. (1989). Electrospray ionization for mass-spectrometry of large biomolecules. *Science*, 246(4926), 64-71.
- Whitesides, G. M., & Grzybowski, B. (2002). Self-assembly at all scales. *Science*, 295(5564), 2418-2421.
- Whitesides, G. M., Mathias, J. P., & Seto, C. T. (1991). Molecular self-assembly and nanochemistry: a chemical strategy for the synthesis of nanostructures: DTIC Document.

- Whitmore, L., & Wallace, B. A. (2008). Protein secondary structure analyses from circular dichroism spectroscopy: methods and reference databases. *Biopolymers*, 89(5), 392-400.
- Zhang, S., Holmes, T., Lockshin, C., & Rich, A. (1993). Spontaneous assembly of a self-complementary oligopeptide to form a stable macroscopic membrane. *Proceedings of the National Academy of Sciences*, 90(8), 3334-3338.
- Zhou, W., & Wang, Z. L. (2007). *Scanning microscopy for nanotechnology: techniques and applications*: Springer science & business media.